Cosmic Neutrinos

Chris Quigg[*]

Fermi National Accelerator Laboratory,
P.O. Box 500, Batavia, Illinois 60510 USA
and
Theory Group, Physics Department,
CERN, CH-1211 Geneva 23, Switzerland

I recall the place of neutrinos in the electroweak theory and summarize what we know about neutrino mass and flavor change. I next review the essential characteristics expected for relic neutrinos and survey what we can say about the neutrino contribution to the dark matter of the Universe. Then I discuss the standard-model interactions of ultrahigh-energy neutrinos, paying attention to the consequences of neutrino oscillations, and illustrate a few topics of interest to neutrino observatories. I conclude with short comments on the remote possibility of detecting relic neutrinos through annihilations of ultrahigh-energy neutrinos at the Z resonance.

I. INTRODUCTION

Neutrinos are abundant, and they infiltrate everything around us—even you and me! Each second, some 10^{14} neutrinos made in the Sun and about a thousand neutrinos made by cosmic rays in Earth's atmosphere pass through your body. Other neutrinos reach us from natural and artificial sources: decays of radioactive elements inside the Earth [1, 2, 3], and emanations from nuclear reactors and particle accelerators. Inside your body are more than 10^7 neutrino relics from the early universe, provided that neutrinos are stable on cosmological time scales. The calculated relic density of neutrinos and antineutrinos in the current universe is $n_{\nu_i 0} = n_{\bar{\nu}_i 0} \approx 56$ cm^{-3} for each flavor. The neutrino gas that we believe permeates the present Universe has never been detected directly. Imaginative schemes have been proposed to record the elastic scattering of the 1.95-K relic neutrinos, but all appear to require significant further technological development before they can approach the needed sensitivity [4, 5, 6]. Because neutrinos have mass, relic neutrinos would constitute some of the dark matter of the universe. Neutrinos as dark matter will be one theme of this lecture. The second major topic will be the interactions of ultrahigh-energy neutrinos and a cursory look at the prospect that neutrino observatories may teach lessons about particle physics [7]. Then we will look briefly at the possibility of detecting the relic neutrinos by observing the resonant annihilation of extremely-high-energy cosmic neutrinos on the background neutrinos through the reaction $\nu\bar{\nu} \to Z^0$.

The background in cosmology that underlies our discussion may be found in §19–23 of the *Review of Particle Physics* [8] or in any modern textbook; Scott Dodelson reviewed the essentials in his course at this school [9]. The monographs by Bahcall [10] and by Giunti & Kim [11] treat many topics in neutrino astrophysics; Steen Hannestad's review article on primordial neutrinos [12] and Gianpiero Mangano's lecture notes [13] encompass cosmological constraints on neutrino properties. The 2007 Neutrino Physics Summer School at Fermilab [14] provided a comprehensive survey of neutrino physics. For a guide to the Russian literature, consult Ref. [15].

According to the standard cosmology, neutrinos should be the most abundant particles in the Universe, after the photons of the cosmic microwave background, provided that they are stable over cosmological times. Because they interact only weakly, neutrinos fell out of equilibrium when the age of the Universe was ≈ 0.1 s (redshift $z \approx 10^{10}$) and the temperature of the Universe was a few MeV. Accordingly, relic neutrinos have been present—as witnesses or participants—for landmark events in the history of the Universe: the era of big-bang nucleosynthesis, a few minutes
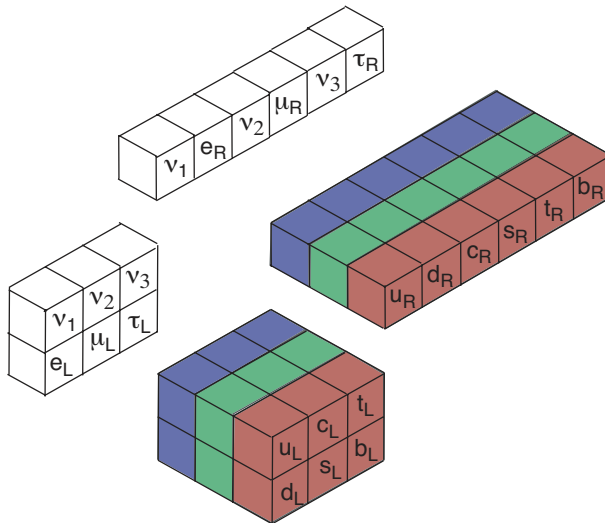
---

[*]Electronic address: quigg@fnal.gov

FIG. 1: Left-handed doublets and right-handed singlets of quarks and leptons that inspire the structure of the electroweak theory.

into the life of the Universe [16, 17]; the decoupling era around 379 000 y [18], when the cosmic microwave background was imprinted on the surface of last scattering; and the era of large-scale structure formation, when the Universe was only a few percent of its current age [19, 20]. For recent quantitative assessments of evidence that neutrinos were present at these times, see Ref. [21, 22, 23].

Some of the earliest cosmological bounds on neutrino masses followed from the requirement that massive relic neutrinos, present today in the expected numbers, do not saturate the critical density of the Universe [24, 25]. Refined analyses, incorporating constraints from a suite of cosmological measurements, sharpen the bounds on the sum of light-neutrino masses [26]. The discovery of neutrino oscillations [27, 28, 29] implies that neutrinos have mass, but we cannot precisely compute the contribution of relic neutrinos to the dark matter of the Universe until we establish the absolute scale of neutrino masses. Current estimates for the neutrino fraction of the Universe's mass–energy density lie in the range $0.1\% \lesssim \Omega_\nu \lesssim$ a few %, under standard assumptions. The uncertainty reflects our incomplete knowledge of neutrino properties.

II.   NEUTRINO INTERACTIONS AND PROPERTIES

A.   Neutrinos in the Electroweak Theory

The electroweak theory emerged through trial and error, guided by experiment. The idealization that neutrinos are massless did not flow from any sound principle, but was inferred from kinematical evidence against measurably large masses. Since fermion mass normally requires linking left-handed and right-handed states, the presumed masslessness of the neutrinos could be captured by the omission of right-handed neutrinos from the theory, consistent with evidence that ν_e [30], ν_μ [31, 32], and (much later) ν_τ[33] produced in charged-current interactions are left-handed. On current evidence, the correct electroweak gauge symmetry melds the $SU(2)_L$ family (weak-isospin) symmetry suggested by the left-handed doublets of Figure 1 with a $U(1)_Y$ weak-hypercharge phase symmetry.[1]

---

[1] See my lectures at the neutrino summer school [34] for an informal but thorough development.

TABLE I: Some properties of the leptons [8].

Lepton	Mass	Lifetime
ν_e	< 2 eV	
e^-	0.510 998 918(44) MeV	> 4.6 × 10²⁶ y (90% CL)
ν_μ	< 0.19 MeV (90% CL)	
μ^-	105.658 369 2(94) MeV	2.197 03(4) × 10⁻⁶ s
ν_τ	< 18.2 MeV (95% CL)	
τ^-	1776.90 ± 0.20 MeV	290.6 ± 1.0 × 10⁻¹⁵ s

We characterize the $\mathrm{SU(2)_L \otimes U(1)_Y}$ theory by the left-handed quarks

$$\mathsf{L}_q^{(1)} = \begin{pmatrix} u \\ d \end{pmatrix}_\mathrm{L} \qquad \mathsf{L}_q^{(2)} = \begin{pmatrix} c \\ s \end{pmatrix}_\mathrm{L} \qquad \mathsf{L}_q^{(3)} = \begin{pmatrix} t \\ b \end{pmatrix}_\mathrm{L} \,, \tag{1}$$

with weak isospin $I = \frac{1}{2}$ and weak hypercharge $Y(\mathsf{L}_q) = \frac{1}{3}$; their right-handed weak-isoscalar counterparts

$$\mathsf{R}_u^{(1,2,3)} = u_\mathrm{R}, c_\mathrm{R}, t_\mathrm{R} \text{ and } \mathsf{R}_d^{(1,2,3)} = d_\mathrm{R}, s_\mathrm{R}, b_\mathrm{R} \,, \tag{2}$$

with weak hypercharges $Y(\mathsf{R}_u) = \frac{4}{3}$ and $Y(\mathsf{R}_d) = -\frac{2}{3}$; the left-handed leptons

$$\mathsf{L}_e = \begin{pmatrix} \nu_e \\ e^- \end{pmatrix}_\mathrm{L} \qquad \mathsf{L}_\mu = \begin{pmatrix} \nu_\mu \\ \mu^- \end{pmatrix}_\mathrm{L} \qquad \mathsf{L}_\tau = \begin{pmatrix} \nu_\tau \\ \tau^- \end{pmatrix}_\mathrm{L} \,, \tag{3}$$

with weak isospin $I = \frac{1}{2}$ and weak hypercharge $Y(\mathsf{L}_\ell) = -1$; and the right-handed weak-isoscalar charged leptons

$$\mathsf{R}_{e,\mu,\tau} = e_\mathrm{R}, \mu_\mathrm{R}, \tau_\mathrm{R} \,, \tag{4}$$

with weak hypercharge $Y(\mathsf{R}_\ell) = -2$. (Weak isospin and weak hypercharge are related to electric charge through $Q = I_3 + \frac{1}{2}Y$.) Right-handed neutrinos are left out.

I do not think that we know enough to specify a new ("ν") standard model,[2] but the inference from neutrino oscillations that neutrinos have mass makes it tempting to suppose that right-handed neutrinos do exist, as indicated in Figure 1. These right-handed neutrinos are sterile—inert with respect to the known interactions with γ, left-handed W, and Z. As we shall see in more detail in § II E, neutrino masses can evade the usual requirement that a (Dirac) fermion mass link left-handed and right-handed states, provided that the neutrino is its own antiparticle. We cannot yet establish the existence of right-handed neutrinos, but I will take their existence as a working hypothesis. Given the absence of detectable right-handed charged-current interactions, it is not surprising that what we surmise about the right-handed neutrinos is of little consequence of most studies of neutrino interactions.

B.   First Look at Neutrino Properties

The leptons are all spin-$\frac{1}{2}$ particles that we idealize as pointlike, in light of experimental evidence that no internal structure can be discerned at a resolution $\lesssim$ few × 10⁻¹⁷ cm. What we know of their masses and lifetimes is gathered in Table I. The *kinematically determined* neutrino masses are consistent with zero; as we shall see in the following

---

[2] Some plausible definitions are explored in Refs. [35, 36].

§ II C, the observation of neutrino oscillations imply that the neutrinos have nonzero, and unequal, masses. The preferred reaction for measuring the mass of the neutrino (mixture) associated with the electron is tritium β-decay,

$$^3\text{H} \rightarrow \ ^3\text{He} \ e^- \ \bar{\nu}_e \ , \tag{5}$$

for which the endpoint energy is $Q \approx 18.57$ keV. Sources of the spectral distortions that limited the sensitivity of early experiments are absent in modern experiments using free tritium. Nevertheless, detecting a small neutrino mass is enormously challenging: the fraction of counts in the beta spectrum for a massless neutrino that lie beyond the endpoint associated with a 1-eV neutrino is but 2×10^{-13} of the total decay rate. The KATRIN experiment [37], which scales up the intensity of the tritium beta source as well as the size and precision of previous experiments by an order of magnitude, is designed to measure the mass of the electron neutrino directly with a sensitivity of 0.2 eV.

Massless neutrinos are stable, but massive neutrinos might decay. Over a distance L, decay would deplete the flux of extremely relativistic neutrinos of energy E, mass m, and lifetime τ by the factor $e^{-L/\gamma c\tau} = \exp\left(-\frac{L}{Ec} \cdot \frac{m}{\tau}\right)$, where c is the speed of light and γ is the Lorentz factor. A limit on depletion thus implies a bound on the reduced neutrino lifetime, τ/m. The most stringent such bound, derived from solar γ- and x-ray fluxes, applies for radiative neutrino decay, $\tau/m > 7 \times 10^9$ s/eV [38, 39]. The present bound on *nonradiative* decays, deduced from the survival of solar neutrinos, is far less constraining: $\tau/m \gtrsim 10^{-4}$ s/eV [40]. We shall have more to say about probing neutrino instability in § III E.

C.   Evidence for Neutrino Oscillations

If neutrinos are massless, we have the freedom to identify the mass eigenstates with flavor eigenstates, so the leptonic weak interactions are flavor preserving: $W^- \rightarrow \ell^- \bar{\nu}_\ell$ and $Z \rightarrow \nu_\ell \bar{\nu}_\ell$, where $\ell = e, \mu, \tau$. A neutrino that moves at the speed of light cannot change character between production and subsequent interaction, so massless neutrinos do not mix.

Time passes for massive neutrinos, which do not move at the speed of light. If neutrinos of definite flavor $(\nu_e, \nu_\mu, \nu_\tau)$ are superpositions of different mass eigenstates (ν_1, ν_2, ν_3), the mass eigenstates evolve in time with different frequencies and so the superposition changes in time: a beam created as flavor ν_α evolves into a flavor mixture. The essential phenomenological framework is well known;[3] we will review just enough to put the observations in context. We achieve an adequate orientation by simplifying to the case of two families.

Suppose that two flavor eigenstates ν_α and ν_β are superpositions of the mass eigenstates ν_i and ν_j, such that

$$\nu_\alpha = \nu_i \cos\theta + \nu_j \sin\theta; \ \ \nu_\beta = -\nu_i \sin\theta + \nu_j \cos\theta \ . \tag{6}$$

The mixing angle θ should be predicted by an eventual theory of fermion masses; for now, it is to be determined experimentally.

After propagating over a distance L, a beam created as ν_α with energy E has a probability to mutate into ν_β given by

$$P_{\alpha \rightarrow \beta} = \sin^2 2\theta \sin^2 \left(\Delta m^2 L/4E \right) \ , \tag{7}$$

where $\Delta m^2 = m_j^2 - m_i^2$. Extending the observations of the KamiokaNDE experiment [45], Super-K has produced very compelling evidence [46] that ν_μ produced in the atmosphere disappear (into other flavors, dominantly ν_τ) during propagation over long distances. Their evidence, in the form of a zenith-angle distribution and the L/E plot, has been confirmed and refined by the long-baseline accelerator experiments K2K [47] and MINOS [48, 49]. The most

---

[3] One convenient reference for this audience is Boris Kayser's course at the 2004 SLAC Summer Institute [41]. The Nobel lectures of Ray Davis [42] and Masatoshi Koshiba [43] are good sources for the history of neutrino oscillation studies. Strumia & Vissani's protobook [44] contains a wealth of experimental information and analysis.
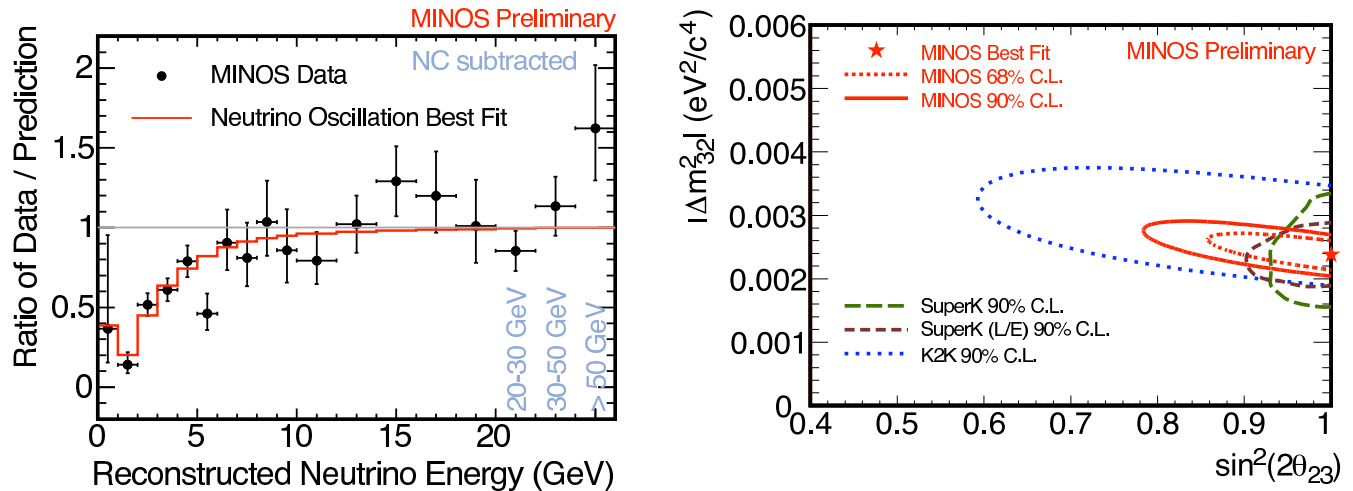
FIG. 2: Left pane: Ratio of the spectrum of neutrino-induced events in the MINOS far detector, with neutral-current events subtracted, to the null-oscillation prediction (points). The best-fit oscillation expectation is overlaid as the solid red curve. Right pane: preliminary MINOS best fit point (star), 68% and 90% CL contours (red), compared with 90% CL contours determined in the Super-Kamiokande zenith angle [46] and L/E analyses [50], as well as that from the K2K experiment [47] [Graphs from Ref. [49]]

recent measurements come from MINOS, some 735 km distant from Fermilab at the Soudan mine in Minnesota. The left pane of Figure 2 shows how their yield of ν_μ events, compared to the no-oscillation expectation, varies with beam energy at fixed baseline—just as anticipated in the oscillation scenario. The right pane of Figure 2 summarizes the constraints on the mixing angle and mass-squared difference from Super-K, K2K, and MINOS. Current evidence is consistent with maximal mixing and $|\Delta m^2| \approx 2.5 \times 10^{-3}$ eV^2.

No appreciable oscillation of atmospheric ν_e has been observed, but flavor change has been observed in neutrinos created in the Sun. Analysis of the solar neutrino experiments is a bit involved, because neutrinos experience matter effects during their journey outward from the production region. The upshot is that the $E_\nu \approx 10$ MeV ^{8}B neutrinos emerge as a nearly pure ν_2 mass eigenstate. Thus, they do not oscillate during the passage from Sun to Earth; the flavor change has already happened within the Sun. The lower energy pp ($E_\nu \approx 200$ keV) and ^{7}Be ($E_\nu \approx 900$ keV) neutrinos are not strongly affected by matter in the Sun, and do undergo oscillations on their Sun–Earth trajectory. The KamLAND reactor experiment [29, 51, 52] has seen a signal for vacuum neutrino oscillations of $\bar{\nu}_e$ that supports and refines the interpretation of the solar neutrino experiments. The Borexino experiment [53] has for the first time detected the ^{7}Be neutrinos, again supporting the oscillation interpretation and parameters.

A deficit of solar neutrinos observed as ν_e, compared with the expectations of the standard solar model, had been a feature of data for some time. Ruling in favor of the oscillation (neutrino-flavor-change) hypothesis, as opposed to a defective solar model, required the combination of several measurements to demonstrate that the missing ν_e are present as ν_μ and ν_τ arriving from the Sun. The solar neutrinos are not energetic enough to initiate $\nu_\mu \to \mu$ or $\nu_\tau \to \tau$ transitions, but indirect means were provided by the Sudbury Neutrino Observatory, SNO, a heavy-water D_2O Cherenkov detector. The deuteron target makes it possible to distinguish three kinds of neutrino interactions sensitive to differently weighted mixtures of ν_e, ν_μ. and ν_τ. The charged-current deuteron dissociation [CC] reaction,

$$\nu_e d \to e^- \, p \, p \,, \tag{8}$$

proceeds by W-boson exchange, and is sensitive only to the ν_e flux. Neutral-current dissociation [NC],

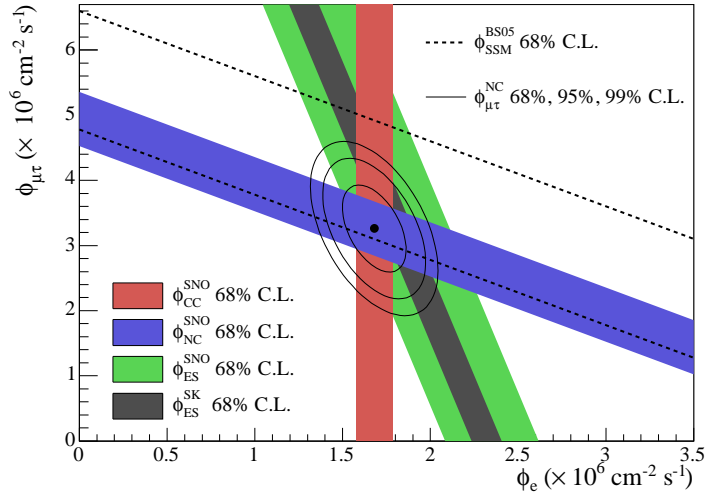$$\nu_\ell d \to \nu_\ell \, p \, n \,, \tag{9}$$

FIG. 3: Flux of $\mu + \tau$ neutrinos versus flux of electron neutrinos determined in solar neutrino experiments. The filled bands indicate the CC, NC and ES flux measurements. The Standard Solar Model [56] predicts that the total ^{8}B solar neutrino flux lies between the dashed lines. The total flux measured with the NC channel is shown as the solid (blue) band parallel to the model prediction. The Super-Kamiokande ES result [57] is the dark narrow band within the (green) SNO ES band. The intercepts of the experimental bands with the axes represent $\pm 1\sigma$ uncertainties. The point represents ϕ_e from the CC flux (red band) and $\phi_{\mu\tau}$ from the NC-CC difference; the contours represent 68%, 95%, and 99% C.L. [From Ref. [58]]

proceeds by Z exchange, and is sensitive to the total flux of active neutrino species $\nu_e + \nu_\mu + \nu_\tau$. Elastic scattering from electrons in the target [ES] is sensitive to a weighted average $\approx \nu_e + \frac{1}{7}(\nu_\mu + \nu_\tau)$ of the active-neutrino fluxes, as we can see by inspecting the cross sections

$$\sigma(\nu_{\mu,\tau} e \rightarrow \nu_{\mu,\tau} e) = \frac{G_F^2 m_e E_\nu}{2\pi} \left[L_e^2 + R_e^2/3 \right] \quad (Z\text{-exchange only})$$

$$\sigma(\nu_e e \rightarrow \nu_e e) = \frac{G_F^2 m_e E_\nu}{2\pi} \left[(L_e + 2)^2 + R_e^2/3 \right] \ (W + Z\text{-exchange}) \tag{10}$$

where the $Ze\bar{e}$ chiral couplings are $L_\ell = 2\sin^2\theta_W - 1 \approx -\frac{1}{2}$ and $R_\ell = 2\sin^2\theta_W \approx \frac{1}{2}$. This reaction can be studied as well in ordinary water-Cherenkov detectors.

Super-K and SNO observations [28, 54, 55] are summarized in Figure 3. Taken together, they indicate that the *total* flux agrees with solar model, but only 30% of neutrinos arrive from the Sun as ν_e. The nonzero value of $\phi_{\mu\tau}$ provides strong evidence that neutrinos created as ν_e are transformed into other active flavors. All the evidence is consistent with the conclusion that ν_e is dominantly a mixture of two mass eigenstates, designated ν_1 and ν_2, with a "solar" mass-squared difference $\Delta m_\odot^2 = m_2^2 - m_1^2 \approx 7.9 \times 10^{-5} \text{ eV}^2$ and mixing angle $\sin^2\theta_\odot \approx 0.3$. No oscillation phenomena have yet been established beyond the "atmospheric" and "solar" sectors [59].

The atmospheric and solar neutrino experiments, with their reactor and accelerator complements, have partially characterized the neutrino spectrum in terms of a closely spaced solar pair ν_1 and ν_2, where ν_1 is taken by convention to be the lighter member of the pair, and a third neutrino, more widely separated in mass. We do not yet know whether ν_3 lies above ("normal hierarchy") or below ("inverted hierarchy") the solar pair, and experiment has not yet set the absolute scale of neutrino masses. Figure 4 shows the normal and inverted spectra as functions of assumed values for the mass of the lightest neutrino.
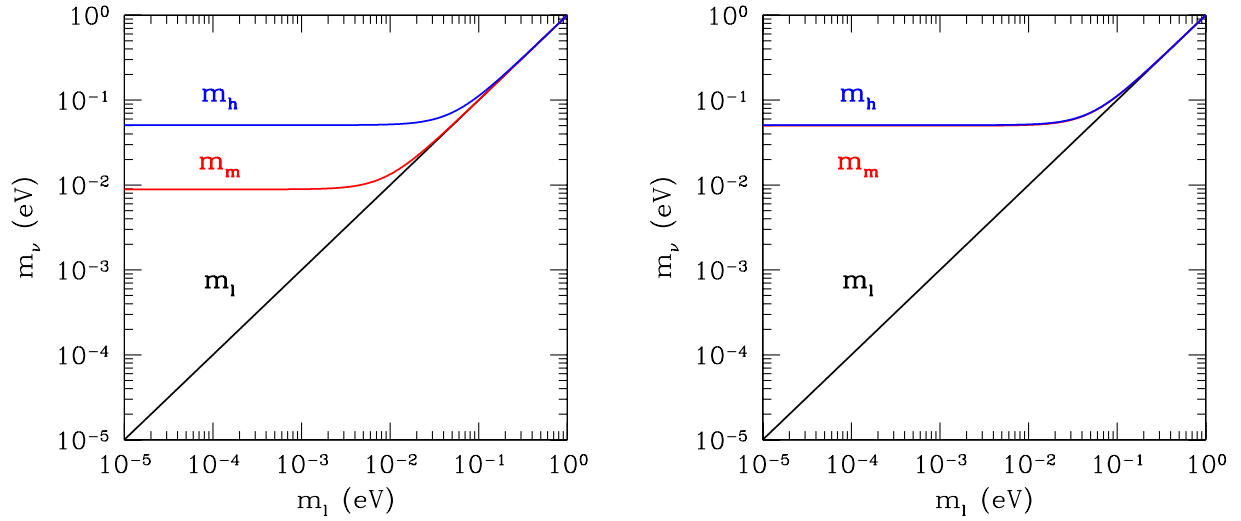
FIG. 4: Favored values for the light, medium, and heavy neutrino masses m_ℓ, m_m, m_h, as functions of the lightest neutrino mass in the three-neutrino oscillation scenario for the normal (left pane) and inverted hierarchy (right pane). We take the solar mass-squared difference to be $\Delta m_\odot^2 = m_2^2 - m_1^2 = 7.9 \times 10^{-5}$ eV^2, and the atmospheric $\Delta m_\mathrm{atm}^2 = |m_3^2 - m_1^2| = 2.5 \times 10^{-3}$ eV^2.

D.   Character of the Relic Neutrino Background

The cosmic microwave background is characterized by a Bose–Einstein blackbody distribution of photons (per unit volume)[4]

$$\frac{dn_\gamma(T)}{d^3 p} = \frac{1}{(2\pi)^3} \frac{1}{\exp{(p/T)} - 1} \;, \tag{11}$$

where p is the relic momentum and T is the temperature of the photon ensemble. The number density of photons throughout the Universe is

$$n_\gamma(T) = \frac{1}{(2\pi)^3} \int d^3 p \, \frac{1}{\exp{(p/T)} - 1} = \frac{2\zeta(3)}{\pi^2} T^3, \tag{12}$$

where $\zeta(3) \approx 1.20205$ is Riemann's zeta function. In the present Universe, with a photon temperature $T_0 = (2.725 \pm 0.002)$ K [18], the photon density is

$$n_{\gamma 0} \equiv n_\gamma(T_0) \approx 410 \text{ cm}^{-3} \;. \tag{13}$$

The present photon density provides a benchmark for other big-bang relics. The essential observation is that neutrinos decoupled when the cosmic soup cooled to around 1 MeV, so did not share in the energy released when electrons and positrons annihilated at $T \approx m_e$, the electron mass. Applying entropy conservation and counting

---

[4] The review article by Steigman [60] is a good introduction to this subject. We adopt units such that $\hbar = 1 = c$, and we will measure temperature in kelvins or electron volts, as appropriate to the situation. The conversion factor is Boltzmann's constant, $k = 8.617343 \times 10^{-5}$ eV K^{-1}.

relativistic degrees of freedom, it follows that the ratio of neutrino and photon temperatures (below m_e) is

$$T_\nu/T = \left(\tfrac{4}{11}\right)^{1/3} , \tag{14}$$

so that the present neutrino temperature is

$$T_{\nu 0} = \left(\tfrac{4}{11}\right)^{1/3} T_0 = 1.945 \text{ K} \rightsquigarrow 1.697 \times 10^{-4} \text{ eV} . \tag{15}$$

The momentum distribution of relic neutrinos follows the Fermi–Dirac distribution (with zero chemical potential),

$$\frac{dn_{\nu_i}(T_\nu)}{d^3p} = \frac{dn_{\nu_i^c}(T_\nu)}{d^3p} = \frac{1}{(2\pi)^3} \frac{1}{\exp{(p/T_\nu)} + 1} . \tag{16}$$

The number distribution of relic neutrinos or antineutrinos is therefore

$$
\begin{aligned}
n_{\nu_i}(T_\nu) &= \frac{1}{(2\pi)^3} \int d^3p \, \frac{1}{\exp{(p/T_\nu)} + 1} \\
&= \frac{3\zeta(3)}{4\pi^2} T_\nu^3 = \tfrac{3}{22} n_\gamma(T) .
\end{aligned}
\tag{17}
$$

In the present Universe, the number density of each (active) neutrino or antineutrino species is[5]

$$n_{\nu_i 0} \equiv n_{\nu_i}(T_{\nu 0}) \approx 56 \text{ cm}^{-3} , \tag{18}$$

plus a 1% correction from reheating effects detailed in [62]. The mean momentum of relic neutrinos today is

$$\langle p_{\nu 0} \rangle = \frac{7}{2} \frac{\zeta(4)}{\zeta(3)} \cdot T_{\nu 0} \approx 3.151 T_{\nu 0} \approx 5.314 \times 10^{-4} \text{ eV} , \tag{19}$$

where we have used $\zeta(4) = \pi^4/90 = 1.08232$. In the same way, the mean-squared neutrino momentum is given by

$$\langle p_{\nu 0}^2 \rangle = 15 \frac{\zeta(5)}{\zeta(3)} \cdot T_{\nu 0}^2 \approx 12.94 \, T_{\nu 0}^2 , \tag{20}$$

so that

$$\langle p_{\nu 0}^2 \rangle^{\frac{1}{2}} \approx 3.597 \, T_{\nu 0} \approx 6.044 \times 10^{-3} \text{ eV} . \tag{21}$$

With our (partial) knowledge of neutrino masses, we can estimate the contribution of neutrinos to the density of the current universe. The left-hand scale of Figure 5 shows the summed neutrino masses $m_1 + m_2 + m_3$ for the normal and inverted hierarchies, as functions of the lightest neutrino mass. The neutrino oscillation data imply that $\sum_i m_{\nu_i} \gtrsim 0.06$ eV in the case of the normal hierarchy, and $\sum_i m_{\nu_i} \gtrsim 0.11$ eV in the case of the inverted hierarchy. Using the calculated number density (18), we can deduce the neutrino contribution to the mass density, expressed in units of the critical density

$$\rho_c \equiv 3H_0^2/8\pi G_N = 1.05h^2 \times 10^4 \text{ eV cm}^{-3} = 5.6 \times 10^3 \text{ eV cm}^{-3} , \tag{22}$$

where we have taken the reduced Hubble constant to be $h = 0.73$. This is measured by the right-hand scale in Figure 5. We find that neutrinos contribute $\Omega_\nu \gtrsim (1.2, 2.2) \times 10^{-3}$ for the (normal, inverted) spectrum, and no more than 10% of critical density, should the lightest neutrino mass approach 1 eV. Combining (22) and (18), we deduce that the condition for neutrinos not to overclose the Universe is[6]

$$\sum_i m_{\nu_i} \lesssim 50 \text{ eV} , \tag{23}$$

---

[5] Unconventional neutrino histories can alter this expectation. These include lepton asymmetries in the early universe, neutrino clustering, and a neutrinoless universe. For a brief survey, with references, see §V of Ref. [61].

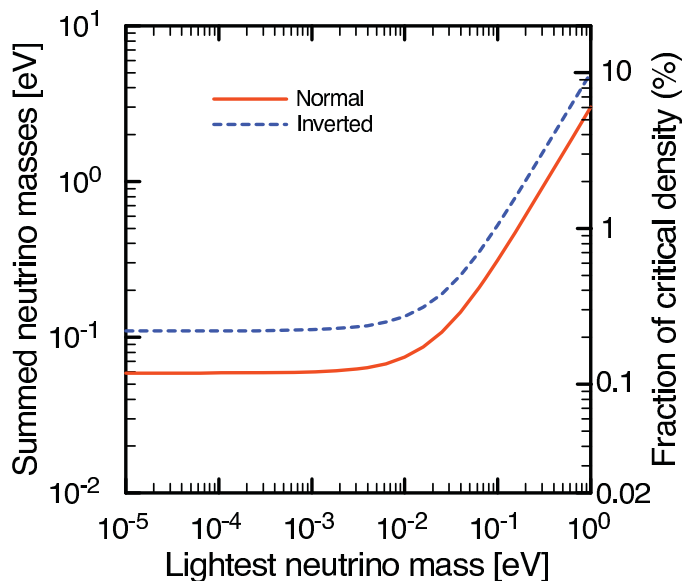[6] This line of argument may be traced to Refs. [24, 25, 63, 64].

FIG. 5: Contributions of relic neutrinos to the mass density of the Universe, as functions of the mass of the lightest neutrino, for the normal (solid line) and inverted (dashed line) mass hierarchies.

so long as neutrinos are stable on cosmological time scales and that the expected neutrino density is not erased by interactions beyond the standard electroweak theory [65].[7]

Neutrinos influence fluctuations in the cosmic microwave background, affect the development of density perturbations that set the pattern of large-scale structure, and modulate the baryon acoustic oscillations. Analyses of the interplay between neutrinos and astronomical observables provide bounds on the sum of neutrino masses, many of which are compiled in Refs. [8, 67, 68, 69, 70]. Depending on the richness of the data set considered and the specificity of the assumed cosmological scenario, recent inferences range from ≈ 1.5 eV [26, 71] to approximately 0.6 eV [26, 71, 72, 73] to $\lesssim 0.2$ eV [73, 74, 75, 76]. These provocative constraints are less secure than the bound (23) derived from $\rho_\nu \lesssim \rho_c$, but they are highly suggestive. It is worth noting that detection of late-time neutrino influence may imply an improved lower bound on the neutrino lifetime [77]. It will be very interesting to watch the evolving conversation between direct measurements and indirect inferences [20, 78, 79].

E.   Fermion masses and mixings

In the standard electroweak theory, fermion mass arises from gauge-invariant Yukawa interactions between the complex scalar fields ϕ introduced to hide the electroweak symmetry and the quarks or charged leptons. For the leptons (ℓ runs over e, μ, τ), the Yukawa term is

$$\mathcal{L}_{\mathrm{Yukawa}-\ell} = -\zeta_\ell \left[(\overline{\mathsf{L}}_\ell \phi)\mathsf{R}_\ell + \overline{\mathsf{R}}_\ell (\phi^\dagger \mathsf{L}_\ell) \right] \ , \tag{24}$$

where the spinors L_ℓ and R_ℓ are defined in (3) and (4); a similar interaction appears for quarks. Self-interactions among the scalars may contrive to hide the gauge symmetry. The "Higgs potential" has the form

$$V(\phi^\dagger \phi) = \mu^2 (\phi^\dagger \phi) + |\lambda| \, (\phi^\dagger \phi)^2. \tag{25}$$

---

[7] Lepton asymmetries in the early universe can lead to neutrino densities in the current Universe far from the standard expectation [66].
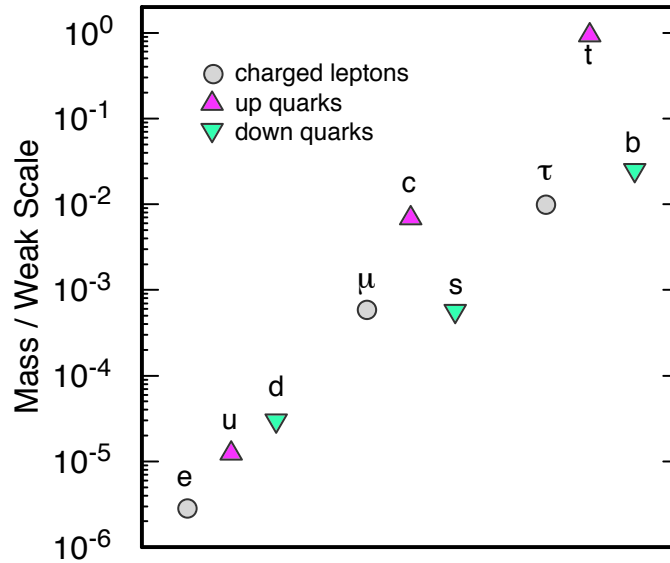
FIG. 6: Yukawa couplings $\zeta_i = m_i/(v/\sqrt{2})$ inferred from the masses of the quarks and charged leptons.

The electroweak symmetry is spontaneously broken if the parameter μ^2 is taken to be negative. In that event, gauge invariance gives us the freedom to choose the state of minimum energy—the vacuum state—to correspond to the vacuum expectation value

$$\langle\phi\rangle_0 = \begin{pmatrix} 0 \\ v/\sqrt{2} \end{pmatrix}, \tag{26}$$

where $v = \sqrt{-\mu^2/|\lambda|} = (G_{\mathrm{F}}\sqrt{2})^{-1/2} \approx 246$ GeV.

When the electroweak symmetry is spontaneously broken, the electron mass emerges as $m_e = \zeta_e v/\sqrt{2}$. Each fermion mass involves a distinct Yukawa coupling ζ. The Yukawa couplings that reproduce the observed quark and charged lepton masses range over many orders of magnitude, as shown in Figure 6. The origin of the Yukawa couplings is obscure: they do not follow from a known symmetry principle, for example. In that sense, therefore, *all fermion masses involve physics beyond the standard model.*

We may seek to accommodate neutrino mass[8] in the electroweak theory by adding to the spectrum a right-handed neutrino N_{R} and constructing the (gauge-invariant) Dirac mass term

$$\mathcal{L}_{\mathrm{D}}^{(\nu)} = -\zeta_\nu \left[(\bar{\mathsf{L}}_\ell \bar{\phi}) N_{\mathrm{R}} + \bar{N}_{\mathrm{R}}(\bar{\phi}^\dagger \mathsf{L}_\ell) \right] \rightarrow -m_{\mathrm{D}} \left[\bar{\nu}_{\mathrm{L}} N_{\mathrm{R}} + \bar{N}_{\mathrm{R}}\nu_{\mathrm{L}} \right] , \tag{27}$$

where $\bar{\phi} = i\sigma_2\phi^*$ is the complex conjugate of the Higgs doublet and $m_{\mathrm{D}} = \zeta_\nu v/\sqrt{2}$. A Dirac mass term conserves the additive lepton number L that takes on the value $+1$ for neutrinos and negatively charged leptons, and -1 for antineutrinos and positively charged leptons. To account for the observed tinyness of the neutrino masses, $m_\nu \lesssim 1$ eV, the Yukawa couplings must be extraordinarily small, $\zeta_\nu \lesssim 10^{-11}$. Whether they are qualitatively more puzzling than the factor of 3×10^5 that separates the electron and top-quark Yukawa couplings is for now a question for intuition.

Matters of taste aside, we have another reason to consider alternatives to the Dirac mass term: unlike all the other particles that enter the electroweak theory, the right-handed neutrinos are standard-model singlets. Alone among the standard-model fermions, they might be their own antiparticles, so-called Majorana fermions. The charge

---

[8] For surveys of attempts to understand neutrino masses, see Refs. [36, 80, 81, 82, 83].

conjugate of a right-handed field is left-handed, $\psi_L^c \equiv (\psi^c)_L = (\psi_R)^c$. Majorana mass terms connect the left-handed and right-handed components of conjugate fields,

$$
\begin{aligned}
-\mathcal{L}_{\mathrm{MA}} &= A(\bar{\nu}_R^c \nu_L + \bar{\nu}_L \nu_R^c) = A\bar{\chi}\chi \\
-\mathcal{L}_{\mathrm{MB}} &= B(\bar{N}_L^c N_R + \bar{N}_R N_L^c) = B\bar{\omega}\omega \ .
\end{aligned}
\tag{28}
$$

The self-conjugate Majorana mass eigenstates are

$$
\begin{aligned}
\chi &\equiv \nu_L + \nu_R^c = \chi^c \\
\omega &\equiv N_R + N_L^c = \omega^c \ .
\end{aligned}
\tag{29}
$$

A Majorana fermion cannot carry any additive quantum number. The mixing of particle and antiparticle fields means that the Majorana mass terms correspond to processes that violate lepton number by two units. Accordingly, the exchange of a Majorana neutrino can mediate neutrinoless double beta decay, $(Z, A) \to (Z + 2, A) + e^- + e^-$. Detecting neutrinoless double beta decay [84, 85, 86, 87] would offer decisive evidence for the Majorana nature of the neutrino.

The mass of the active ν_L may be generated by a Higgs triplet that acquires a vacuum expectation value [88], or by an effective operator that involves two Higgs doublets combined to transform as a triplet [89].

It is interesting to consider both Dirac and Majorana terms, and specifically to examine the case in which Majorana masses corresponding to an active state χ and a sterile state ω arise from weak triplets and singlets, respectively, with masses M_3 and M_1. The neutrino mass matrix then has the form

$$
(\ \bar{\nu}_L \ \ \bar{N}_L^c \ )
\begin{pmatrix} M_3 & m_D \\ m_D & M_1 \end{pmatrix}
\begin{pmatrix} \nu_R^c \\ N_R \end{pmatrix} \ .
\tag{30}
$$

In the highly popular seesaw limit [90, 91, 92, 93, 94], with $M_3 = 0$ and $m_D \ll M_1$, diagonalizing the mass matrix (30) yields two Majorana neutrinos,

$$
n_{1L} \approx \nu_L - \frac{m_D}{M_1} N_L^c \qquad n_{2L} \approx N_L^c + \frac{m_D}{M_1} \nu_L \ ,
\tag{31}
$$

with masses

$$
m_1 \approx \frac{m_D^2}{M_1} \ll m_D \qquad m_2 \approx M_1 \ .
\tag{32}
$$

The seesaw produces one very heavy "neutrino" and one neutrino much lighter than a typical quark or charged lepton. Many alternative explanations of the small neutrino masses have been explored in the literature [95], including some in which collider experiments exploring the Fermi scale could reveal the origin of neutrino masses [96].

The charged-current interactions among the left-handed leptonic mass eigenstates $\boldsymbol{\nu} = (\nu_1, \nu_2, \nu_3)$ and $\boldsymbol{\ell}_L = (e_L, \mu_L, \tau_L)$ are specified by

$$
\mathcal{L}_{\mathrm{CC}}^{(q)} = -\frac{g}{\sqrt{2}} \bar{\boldsymbol{\nu}}\, \gamma^\mu \mathcal{V}^\dagger \boldsymbol{\ell}_L W_\mu^+ + \ \text{h.c.} \ ,
\tag{33}
$$

where the neutrino mixing matrix [97], sometimes called the Pontecorvo [98]–Maki-Nakagawa-Sakata [99] (PMNS) matrix in tribute to neutrino-oscillation pioneers, is

$$
\mathcal{V} =
\begin{pmatrix}
\mathcal{V}_{e1} & \mathcal{V}_{e2} & \mathcal{V}_{e3} \\
\mathcal{V}_{\mu1} & \mathcal{V}_{\mu2} & \mathcal{V}_{\mu3} \\
\mathcal{V}_{\tau1} & \mathcal{V}_{\tau2} & \mathcal{V}_{\tau3}
\end{pmatrix} \ .
\tag{34}
$$

A recent global fit [100] yields the following ranges for the magnitudes of the neutrino mixing matrix elements:

$$
|\mathcal{V}| =
\begin{pmatrix}
0.79 - 0.88 & 0.47 - 0.61 & < 0.20 \\
0.19 - 0.52 & 0.42 - 0.73 & 0.58 - 0.82 \\
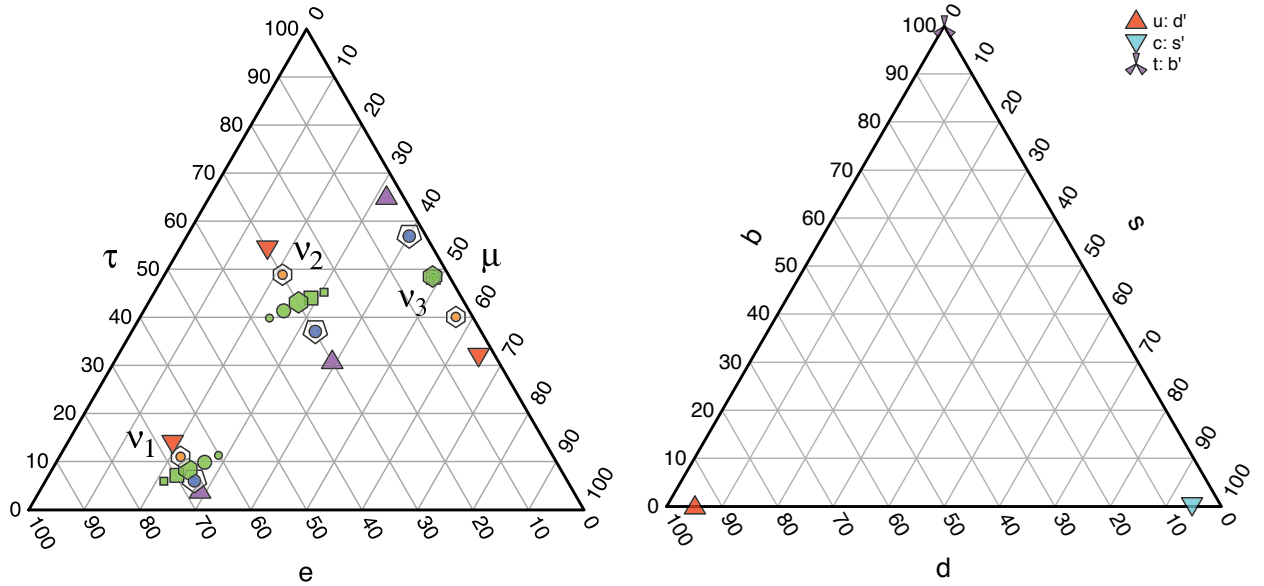0.20 - 0.53 & 0.44 - 0.74 & 0.56 - 0.81
\end{pmatrix} \ .
\tag{35}
$$

FIG. 7: Left pane: ν_e, ν_μ, ν_τ flavor content of the neutrino mass eigenstates ν_1, ν_2, ν_3. The green hexagons denote central values, with $\delta = 0$ and $\theta_{13} = 10°$. Variations in the atmospheric angle θ_{23} are indicated by the points arrayed roughly parallel to the μ scale. Variations in the solar angle θ_{12} are depicted by the green symbols arrayed roughly perpendicular to the μ scale. Right pane: d, s, b composition of the quark flavor eigenstates d' ($\triangle$), s' ($\triangledown$), b' (tripod).

It is conventional to factor the neutrino mixing matrix as

$$\mathcal{V} = \begin{bmatrix} 1 & 0 & 0 \\ 0 & c_{23} & s_{23} \\ 0 & -s_{23} & c_{23} \end{bmatrix} \begin{bmatrix} c_{13} & 0 & s_{13}e^{-i\delta} \\ 0 & 1 & 0 \\ s_{13}e^{i\delta} & 0 & c_{13} \end{bmatrix} \begin{bmatrix} c_{12} & s_{12} & 0 \\ -s_{12} & c_{12} & 0 \\ 0 & 0 & 1 \end{bmatrix} \tag{36}$$

where we abbreviate $s_{ij} = \sin\theta_{ij}$, $c_{ij} = \cos\theta_{ij}$, and δ is a CP-violating phase.

Global fits [100, 101, 102] restrict the mixing parameters to the ranges $30° \lesssim \theta_{12} \lesssim 38°$ for solar oscillations,[9] $35° \lesssim \theta_{23} \lesssim 55°$ for atmospheric oscillations, $\theta_{13} \lesssim 10°$, and leave δ unconstrained. These parameter ranges lead to the flavor content of the neutrino mass eigenstates depicted in the left pane of Figure 7, where central values (fixing $\delta = 0$ and $\theta_{13} = 10°$) are indicated by the green hexagons. We observe that ν_3 consists of nearly equal parts of ν_μ and ν_τ, perhaps with a trace of ν_e, while ν_2 contains similar amounts of ν_e, ν_μ, and ν_τ, and ν_1 is rich in ν_e, with approximately equal minority parts of ν_μ and ν_τ. The observed structure of the neutrino mixing matrix differs greatly from the pattern of the more familiar (Cabibbo–Kobayashi–Maskawa) quark mixing matrix, which is displayed graphically in the right pane of Figure 7.

III. NEUTRINO OBSERVATORIES

A. Generalities

An early goal of the next generation of neutrino telescopes will be to detect the flux of cosmic neutrinos that we believe will begin to show itself above the atmospheric-neutrino background at energies of a few TeV [103]. A short

---

[9] The latest KamLAND analysis [52] tightens this constraint to $33° \lesssim \theta_{12} \lesssim 36°$.

summary of the science program of these instruments is to prospect for cosmic-neutrino sources, to characterize those sources, to study neutrino properties, and to be sensitive to new phenomena in particle physics [7, 104, 105]. The expected sources include active galactic nuclei (AGN) at typical distances of roughly 100 Mpc $\approx 3.1 \times 10^{24}$ m. If neutrinos are produced there in the decay of pions created in pp or $p\gamma$ collisions, then we anticipate—at the source— equal numbers of neutrinos and antineutrinos, with a flavor mix $2\gamma + 2\nu_\mu + 2\bar{\nu}_\mu + 1\nu_e + 1\bar{\nu}_e$, provided that all pions and their daughter muons decay. I denote this standard flux at the source by $\Phi_{\text{std}}^0 = \{\varphi_e^0 = \frac{1}{3}, \varphi_\mu^0 = \frac{2}{3}, \varphi_\tau^0 = 0\}$.

We expect that a neutrino observatory with an instrumented volume of 1 km^3 will be able to survey the cosmic-neutrino flux over a broad range of energies, principally by detecting the charged-current interaction $(\nu_\mu, \bar{\nu}_\mu)N \rightarrow (\mu^-, \mu^+)$ + anything. Important open questions are whether we can achieve efficient, calibrated $(\nu_e, \bar{\nu}_e)$ and $(\nu_\tau, \bar{\nu}_\tau)$ detection, and whether we can record and determine the energy of neutral-current events. Adding these capabilities will enhance the scientific potential of neutrino observatories.

B.   Deeply inelastic scattering

The cross section for deeply inelastic scattering on an isoscalar nucleon may be written in terms of the Bjorken scaling variables $x = Q^2/2M\nu$ and $y = \nu/E_\nu$ as

$$\frac{d^2\sigma}{dxdy} = \frac{2G_F^2 ME_\nu}{\pi} \left(\frac{M_W^2}{Q^2 + M_W^2} \right)^2 \left[xq(x, Q^2) + x\bar{q}(x, Q^2)(1 - y)^2 \right] , \tag{37}$$

where $-Q^2$ is the invariant momentum transfer between the incident neutrino and outgoing muon, $\nu = E_\nu - E_\mu$ is the energy loss in the lab (target) frame, M and M_W are the nucleon and intermediate-boson masses, and $G_F = 1.16632 \times 10^{-5}$ GeV^{-2} is the Fermi constant. The parton densities are

$$\begin{aligned} q(x, Q^2) &= \frac{u_v(x, Q^2) + d_v(x, Q^2)}{2} + \frac{u_s(x, Q^2) + d_s(x, Q^2)}{2} \\ &\quad + s_s(x, Q^2) + b_s(x, Q^2) \end{aligned} \tag{38}$$

$$\bar{q}(x, Q^2) = \frac{u_s(x, Q^2) + d_s(x, Q^2)}{2} + c_s(x, Q^2) + t_s(x, Q^2),$$

where the subscripts v and s label valence and sea contributions, and u, d, c, s, t, b denote the distributions for various quark flavors in a *proton*. The W-boson propagator, which has a negligible effect at low energies, modulates the high-energy cross section and has important consequences for the way the cross section is composed.

I was drawn to this problem by the observation [106] that the W-boson propagator squeezes the significant contributions of the parton distributions toward smaller values of x with increasing energy. There the QCD-induced growth of the small-x parton distribution enhances the high-energy cross section. This stands in contrast to the familiar effect of QCD evolution at laboratory energies, which is to diminish the total cross section as the valence distribution is degraded at high values of Q^2. At that moment, my colleagues and I had developed for our study of supercollider physics [107] the first all-flavor set of parton distributions appropriate for applications at small x and large Q^2, so I had in my hands everything needed for a modern calculation of the charged-current cross section at ultrahigh energies. In a sequence of works on the problem [108, 109, 110, 111], we have tracked the evolving experimental understanding of parton distributions and investigated many facets of ultrahigh-energy neutrino interactions.

Let us recall some of the principal lessons. The valence contribution, which dominates at laboratory energies, becomes negligible above about 10^{16} eV, whereas strange- and charm-quark contributions become significant. Contributions from small values of x become increasingly prominent as the neutrino energy increases. At $E_\nu = 10^5$ GeV, nearly all of the cross section comes from $x \gtrsim 10^{-3}$, but by $E_\nu = 10^9$ GeV, nearly all of the cross section lies below $x = 10^{-5}$, where we lack direct experimental information. Reno has given a comprehensive review of small-x
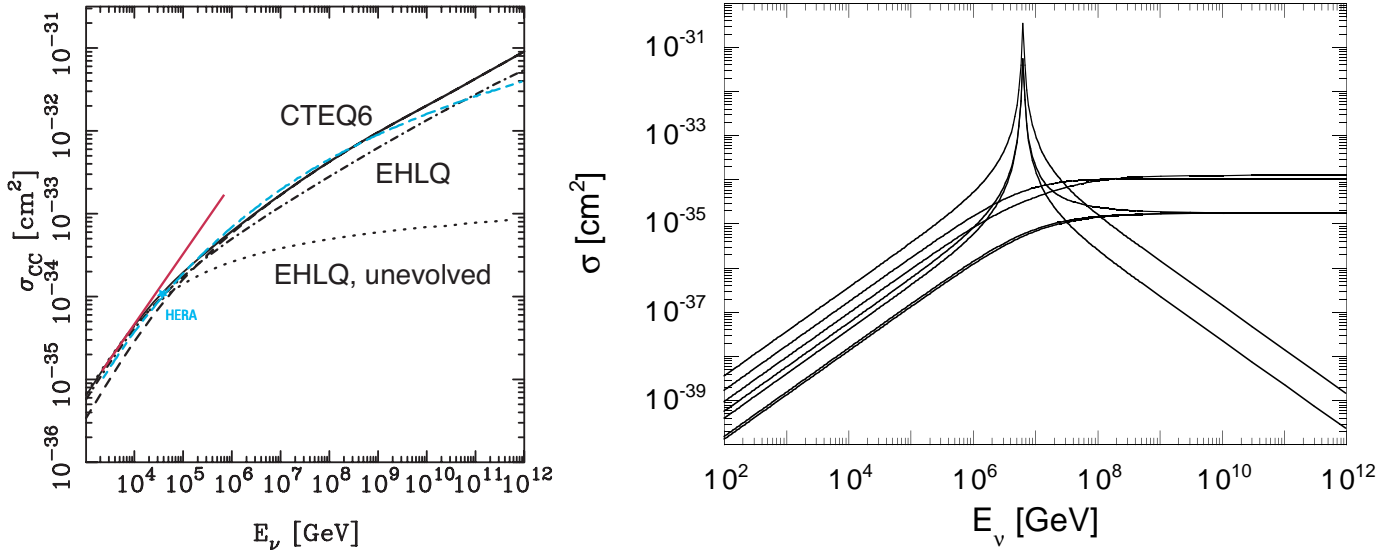
FIG. 8: Left pane: The solid curve shows the charged-current νN cross section calculated using the CTEQ6 parton distributions [114]; the dash-dotted line shows the situation in 1986, using Set 2 of the EHLQ parton distributions [107]. The dotted curve shows the energy dependence of the cross section without QCD evolution, i.e., with the EHLQ distributions frozen at $Q^2 = 5$ GeV^2 [112]. The long-short dashed curve shows the prediction of a structure function that satisfies the Froissart bound for very low x and very large Q^2 [115]. Right pane: Cross sections for neutrino interactions on electron targets. At low energies, from largest to smallest cross section, the processes are (i) $\bar{\nu}_e e \rightarrow$ hadrons, (ii) $\nu_\mu e \rightarrow \mu \nu_e$, (iii) $\nu_e e \rightarrow \nu_e e$, (iv) $\bar{\nu}_e e \rightarrow \bar{\nu}_\mu \mu$, (v) $\bar{\nu}_e e \rightarrow \bar{\nu}_e e$, (vi) $\nu_\mu e \rightarrow \nu_\mu e$, (vii) $\bar{\nu}_\mu e \rightarrow \bar{\nu}_\mu e$ [110].

uncertainties and the possible influence of new phenomena on the total cross section [112].[10]

The left pane of Figure 8 compares our first calculation, using the 1984 EHLQ structure functions, with the modern CTEQ6 parton distributions [114]. At the highest energies plotted, the cross section is about $1.8\times$ our original estimates, because today's parton distributions rise more steeply at small x than did those of two decades ago. HERA measurements have provided the decisive new information [116, 117, 118]. At 10^{12} GeV, the QCD enhancement of the small-x parton density has increased the cross section sixty-fold over the parton-model prediction without evolution. An ongoing concern, addressed in recent studies [115, 119], is whether the density of "wee" partons becomes so large at relevant values of Q^2 that recombination or saturation effects suppress small-x cross sections. HERA measurements of the charged-current reaction $ep \rightarrow \nu +$ anything at an equivalent lab energy near 40 TeV observe the damping due to the W-boson propagator and agree with standard-model. The right pane of Figure 8 shows the interaction cross section for neutrinos on electrons in the Earth, which is generally several orders of magnitude longer than the νN interaction length. An important exception is the $\bar{\nu}_e e \rightarrow W^-$ resonance at $E_\nu \approx 6 \times 10^{15}$ eV.

The rising cross sections have important implications for neutrino telescopes. Figure 9 shows that the Earth is opaque to neutrinos with energies above 40 TeV. This means that the strategy of looking down to distinguish charged-current interactions from the rain of cosmic-ray muons needs to be modified at high energies. On the other hand, the Universe at large is so exceptionally poor in nucleons (only one in every 4 m^3 on average), and so the (νN) interaction length of ultrahigh-energy neutrinos in the cosmos is effectively infinite: a path of 8×10^5 Mpc in the current Universe has a depth of only 1 cmwe.

---

[10] For a new calculation based on the ZEUS-S global fits and incorporating heavy-quark threshold corrections, see Ref. [113].
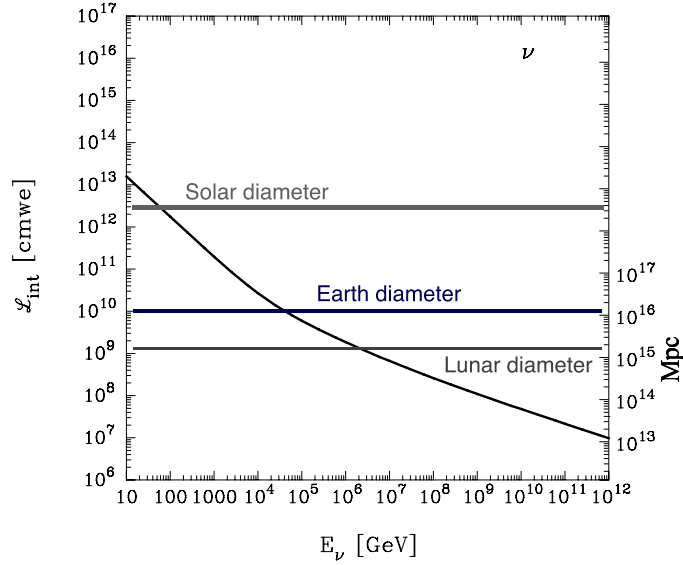
FIG. 9: Interaction length $\mathcal{L}_{\mathrm{int}}^{\nu N} = 1/\sigma_{\nu N}(E_\nu)N_{\mathrm{A}}$, where N_{A} is Avogadro's number, for the reactions $\nu N \rightarrow$ anything as a function of the incident neutrino energy. The left-hand scale, in cmwe, is appropriate for terrestrial applications; the right-hand scale, in Mpc for the current Universe, is appropriate for transport over cosmological distances [61, 111].

C.   Influence of Neutrino Oscillations

In the early days of planning for neutrino telescopes, people noticed that observing τ production through the double-bang signature [120] might provide evidence for neutrino oscillations, since—to good approximation—no ν_τ are produced in conventional sources of ultrahigh-energy neutrinos. The discovery of neutrino oscillations is of course already made; the phenomenon of neutrino oscillations means that the flavor mixture at Earth, $\Phi = \{\varphi_e, \varphi_\mu, \varphi_\tau\}$, will be different from the source mixture $\Phi^0 = \{\varphi_e^0, \varphi_\mu^0, \varphi_\tau^0\}$. The essential fact is that the vacuum oscillation length is very short, in cosmic terms. For $|\Delta m^2| = 10^{-5}$ eV^2, the oscillation length

$$\mathcal{L}_{\mathrm{osc}} = 4\pi E_\nu / |\Delta m^2| \approx 2.5 \times 10^{-24} \text{ Mpc} \cdot (E_\nu/1 \text{ eV}) \tag{39}$$

is a fraction of a megaparsec, even for $E_\nu = 10^{20}$ eV. Accordingly, neutrinos oscillate many times between cosmic source and terrestrial detector.

Neutrinos in the flavor basis $|\nu_\alpha\rangle$ are connected to the mass eigenstates $|\nu_i\rangle$ by the unitary mixing matrix (34), as $|\nu_\alpha\rangle = \sum_i \mathcal{V}_{\beta i}|\nu_i\rangle$. It is convenient to idealize $\sin\theta_{13} = 0$, $\sin 2\theta_{23} = 1$, and consider

$$\mathcal{V}_{\mathrm{ideal}} = \begin{pmatrix} c_{12} & s_{12} & 0 \\ -s_{12}/\sqrt{2} & c_{12}/\sqrt{2} & 1/\sqrt{2} \\ s_{12}/\sqrt{2} & -c_{12}/\sqrt{2} & 1/\sqrt{2} \end{pmatrix} . \tag{40}$$

Then the transfer matrix $\mathcal{X}$ that maps the source flux Φ^0 into the flux at Earth Φ takes the form

$$\mathcal{X}_{\mathrm{ideal}} = \begin{pmatrix} 1-2x & x & x \\ x & \frac{1}{2}(1-x) & \frac{1}{2}(1-x) \\ x & \frac{1}{2}(1-x) & \frac{1}{2}(1-x) \end{pmatrix} , \tag{41}$$

where $x = \sin^2\theta_{12}\cos^2\theta_{12}$. Because the second and third rows are identical, the ν_μ and ν_τ fluxes that result from
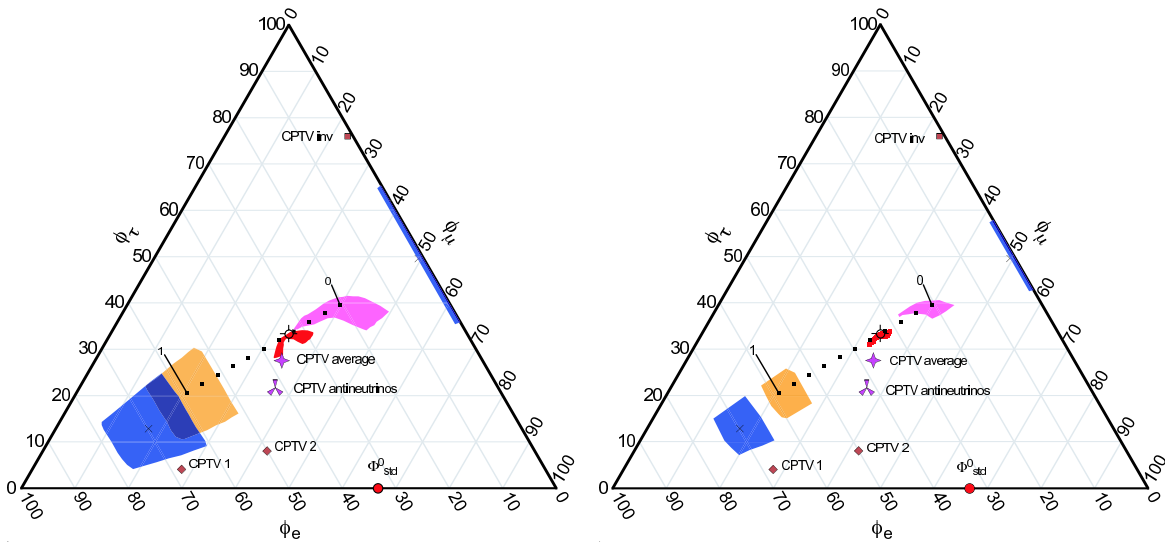
FIG. 10: Ternary plots of the neutrino flux Φ at Earth, showing the implications of current (left pane) and future (right pane) knowledge of neutrino mixing. The small black squares indicate the ν_e fractions produced by the idealized transfer matrix $\mathcal{X}_{\mathrm{ideal}}$ as φ_e^0 varies from 0 to 1 in steps of 0.1. A crossed circle marks the standard mixed spectrum at Earth, $\Phi_{\mathrm{std}} = \{\frac{1}{3}, \frac{1}{3}, \frac{1}{3}\}$; for comparison, a red dot marks the standard source spectrum, $\Phi_{\mathrm{std}}^0 = \{\frac{1}{3}, \frac{2}{3}, 0\}$. Colored swaths delimit the fluxes at Earth produced by neutrino oscillations from the source mixtures (right to left) $\Phi_0^0 = \{0, 1, 0\}$ (pink), Φ_{std}^0 (red), and $\Phi_1^0 = \{1, 0, 0\}$ (orange), using 95% CL ranges for the oscillation parameters. Black crosses ($\times$) show the mixtures at Earth that follow from neutrino decay, assuming normal ($\varphi_e \approx 0.7$) and inverted ($\varphi_e \approx 0$) mass hierarchies. The blue bands at far left show how current and future uncertainties blur the predictions for neutrino decays. The violet tripod indicates how CPT-violating oscillations shape the mix of antineutrinos that originate in a standard source mixture, and the violet cross averages that $\bar{\nu}$ mixture with the standard neutrino mixture. The brown squares denote consequences of CPT violation for antineutrino decays [122].

any source mixture Φ^0 are equal: $\varphi_\mu = \varphi_\tau$. Independent of the value of x, $\mathcal{X}_{\mathrm{ideal}}$ maps $\Phi_{\mathrm{std}}^0 \to \{\frac{1}{3}, \frac{1}{3}, \frac{1}{3}\}$. [11]

The variation of φ_e with the ν_e source fraction φ_e^0 is shown as a sequence of small black squares (for $\varphi_e^0 = 0, 0.1, \ldots, 1$) in Figure 10 for the value $x = 0.21$, which corresponds to $\theta_{12} = 0.57$, the central value in a recent global analysis [121]. The ν_e fraction at Earth ranges from 0.21, for $\varphi_e^0 = 0$, to 0.59, for $\varphi_e^0 = 1$.

The simple analysis based on $\mathcal{X}_{\mathrm{ideal}}$ is useful for orientation, but it is important to explore the range of expectations implied by global fits to neutrino-mixing parameters. We take [122] $0.49 < \theta_{12} < 0.67$, $\frac{\pi}{4} \times 0.8 < \theta_{23} < \frac{\pi}{4} \times 1.2$, and $0 < \theta_{13} < 0.1$. With current uncertainties in the oscillation parameters, a standard source spectrum, $\Phi_{\mathrm{std}}^0 = \{\frac{1}{3}, \frac{2}{3}, 0\}$, is mapped by oscillations onto the red boomerang near $\Phi_{\mathrm{std}} = \{\frac{1}{3}, \frac{1}{3}, \frac{1}{3}\}$ in the left pane of Figure 10. Given that $\mathcal{X}_{\mathrm{ideal}}$ maps $\Phi_{\mathrm{std}}^0 \to \Phi_{\mathrm{std}}$ for any value of θ_{12}, it does not come as a great surprise that the target region is of limited extent. The variation of θ_{23} away from $\frac{\pi}{4}$ breaks the identity $\varphi_\mu \equiv \varphi_\tau$ of the idealized analysis.

One goal of neutrino observatories will be to characterize cosmic sources by determining the source mix of neutrino flavors. It is therefore of interest to examine the outcome of different assumptions about the source. We show in the left pane of Figure 10 the mixtures at Earth implied by current knowledge of the oscillation parameters for source fluxes $\Phi_0^0 = \{0, 1, 0\}$ (the purple band near $\varphi_e \approx 0.2$) and $\Phi_1^0 = \{1, 0, 0\}$ (the orange band near $\varphi_e \approx 0.6$). For the Φ_{std}^0 and Φ_1^0 source spectra, the uncertainty in θ_{12} is reflected mainly in the variation of φ_e, whereas the uncertainty in θ_{23} is expressed in the variation of φ_μ/φ_τ For the Φ_0^0 case, the influence of the two angles is not so orthogonal. For all the source spectra we consider, the uncertainty in θ_{13} has little effect on the flux at Earth. The extent of the three regions, and the absence of a clean separation between the regions reached from Φ_{std}^0 and Φ_0^0 indicates that

---

[11] I owe this formulation to Stephen Parke.
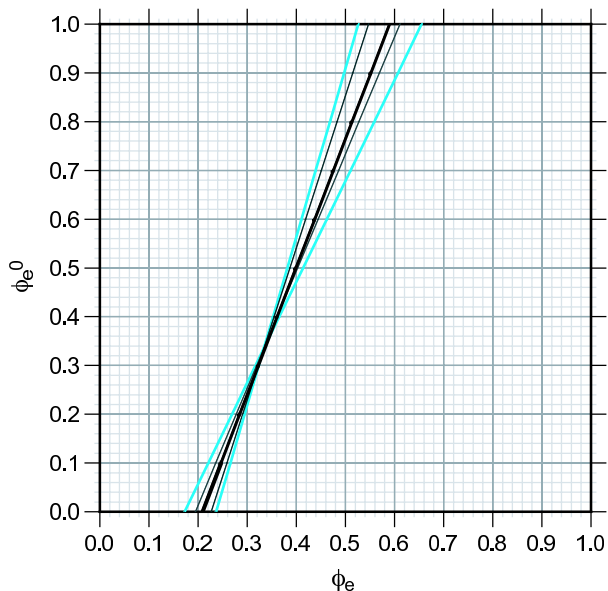
FIG. 11: The source flux φ_e^0 of electron neutrinos reconstructed from the ν_e flux φ_e at Earth, using the ideal transfer matrix $\mathcal{X}_{\mathrm{ideal}}$ of Eqn. (41). The heavy solid line refers to $\theta_{12} = 0.57$. The light blue lines refer to the current experimental constraints (at 95% CL), and the thin solid lines refer to a projection of future experimental constraints [122].

characterizing the source flux will be challenging, in view of the current uncertainties of the oscillation parameters.

We anticipated improved information on θ_{12} and θ_{23} from KamLAND and the long-baseline accelerator experiments at Soudan and Gran Sasso roughly on the time scale on which large-volume neutrino telescopes will come into operation. We based our projections for the future on the ranges $0.54 < \theta_{12} < 0.63^{12}$ and $\frac{\pi}{4} \times 0.9 < \theta_{23} < \frac{\pi}{4} \times 1.1$, still with $0 < \theta_{13} < 0.1$. The results are shown in the right pane of Figure 10. The (purple) target region for the source flux Φ_0^0 shrinks appreciably and separates from the (red) region populated by Φ_{std}^0, which is now tightly confined around Φ_{std}. The (orange) region mapped from the source flux Φ_1^0 by oscillations shrinks by about a factor of two in the φ_e and $\varphi_\mu - \varphi_\tau$ dimensions.

D. Reconstructing the Neutrino Mixture at the Source

What can observations of the blend Φ of neutrinos arriving at Earth tell us about the source [122]? Inferring the nature of the processes that generate cosmic neutrinos is more complicated than it would be if neutrinos did not oscillate. Because ν_μ and ν_τ are fully mixed—and thus enter identically in $\mathcal{X}_{\mathrm{ideal}}$—it is not possible fully to characterize Φ^0. We can, however, reconstruct the ν_e fraction at the source as $\varphi_e^0 = (\varphi_e - x)/(1 - 3x)$, where $x = \sin^2 \theta_{12} \cos^2 \theta_{12}$. The reconstructed source flux φ_e^0 is shown in Figure 11 as a function of the ν_e flux at Earth. The heavy solid line represents the best-fit value for θ_{12}; the light blue lines and thin solid lines indicate the current and future 95% CL bounds on θ_{12}.

A possible strategy for beginning to characterize a source of cosmic neutrinos might proceed by measuring the ν_e/ν_μ ratio and estimating φ_e under the plausible assumption—later to be checked—that $\varphi_\mu = \varphi_\tau$. Very large ($\varphi_e \gtrsim 0.65$) or very small ($\varphi_e \lesssim 0.15$) ν_e fluxes cannot be accommodated in the standard neutrino-oscillation picture. Observing an extreme ν_e fraction would implicate unconventional physics.

Determining the energy dependence of φ_e^0 may also be of astrophysical interest [123]. In a thick source, the highest

---

[12] The latest KamLAND + solar-neutrino analysis does even better: $0.575 < \theta_{12} < 0.63$ [52].

energy muons may interact and lose energy before they can decay. In the limit of $\varphi_e^0 = 0$, the arriving flux will be $\Phi = \{x, \frac{1}{2}(1-x), \frac{1}{2}(1-x)\} \approx \{0.22, 0.39, 0.39\}$ (cf. Figure 10). More generally, measured ν_e fractions that depart significantly from the canonical $\varphi_e = \frac{1}{3}$ would suggest neutrino sources that are in some way nonstandard. An observed flux $\varphi_e = 0.5 \pm 0.1$ points to a source flux $0.47 \lesssim \varphi_e^0 \lesssim 1$, with current uncertainties, whereas $\varphi_e = 0.25 \pm 0.10$ indicates $0 \lesssim \varphi_e^0 \lesssim 0.35$.

Constraining the source flux sufficiently to test the nature of the neutrino production process will require rather precise determinations of the neutrino flux at Earth. Suppose we want to test the idea that the source flux has the standard composition Φ_{std}^0. With today's uncertainty on θ_{12}, a 30% measurement that locates $\varphi_e = 0.33 \pm 0.10$ implies only that $0 \lesssim \varphi_e^0 \lesssim 0.68$. For a measured flux in the neighborhood of $\frac{1}{3}$, the uncertainty in the solar mixing angle is of little consequence: the constraint that arises if we assume the central value of θ_{12} is not markedly better: $0.06 \lesssim \varphi_e^0 \lesssim 0.59$. A 10% measurement of the ν_e fraction, $\varphi_e = 0.33 \pm 0.033$, would make possible a rather restrictive constraint on the nature of the source. The central value for θ_{12} leads to $0.26 \lesssim \varphi_e^0 \lesssim 0.43$, blurred to $0.22 \lesssim \varphi_e^0 \lesssim 0.45$ with current uncertainties.

E. Influence of Neutrino Decays

To this point, we have considered the neutrinos to be stable particles. "Invisible" decays, such as the decay of a heavy neutrino into a lighter neutrino plus a very light—or massless—(pseudo)scalar boson such as the majoron [124, 125] are not very well constrained by observations [40, 126]. [A majoron too massive to serve as a neutrino decay product can nevertheless have important consequences for cosmology, including deviations from the standard expectations for the radiation energy density and changes in the positions of peaks in the cosmic microwave background power spectrum [127].] If CPT invariance holds, SN1987a data set an upper limit on the lifetime of the lightest neutrino of $\tau_\ell/m_\ell \gtrsim 10^5$ s/eV. Observations of solar neutrinos lead to $\tau_2/m_2 \gtrsim 10^{-4}$ s/eV. Finally, if the neutrino spectrum is normal, the data on atmospheric neutrinos coming upward through the Earth, imply $\tau_3/m_3 \gtrsim 10^{-10}$ s/eV.

These rather modest limits open the possibility that some neutrinos do not survive the journey from astrophysical sources. Decays of unstable neutrinos over cosmic distances can lead to mixtures at Earth that are incompatible with the oscillations of stable neutrinos [40, 122, 126]. The candidate decays are transitions between mass eigenstates by emission of a very light particle, $\nu_i \to (\nu_j, \bar{\nu}_j) + X$. Dramatic effects occur when the decaying neutrinos disappear, either by decay to invisible products or by decay into active neutrino species so degraded in energy that they contribute negligibly to the total flux at the lower energy.

If the lifetimes of the unstable mass eigenstates are short compared with the flight time from source to Earth, all the unstable neutrinos will decay, and the (unnormalized) flavor ν_α flux at Earth will be $\widetilde{\varphi}_\alpha(E_\nu) = \sum_{i=\text{stable}} \sum_\beta \varphi_\beta^0(E_\nu)|U_{\beta i}|^2 |U_{\alpha i}|^2$, with $\varphi_\alpha = \widetilde{\varphi}_\alpha / \sum_\beta \widetilde{\varphi}_\beta$. Should only the lightest neutrino survive, the flavor mix of neutrinos arriving at Earth is determined by the flavor composition of the lightest mass eigenstate, *independent of the flavor mix at the source.*

For a normal mass hierarchy $m_1 < m_2 < m_3$, the ν_α flux at Earth is $\varphi_\alpha = |U_{\alpha 1}|^2$. Consequently, the neutrino flux at Earth is $\Phi_{\text{normal}} = \{|U_{e1}|^2, |U_{\mu1}|^2, |U_{\tau1}|^2\}$. If the mass hierarchy is inverted, $m_2 > m_1 > m_3$, the lightest (hence, stable) neutrino is ν_3, so the flavor mix at Earth is determined by $\varphi_\alpha = |U_{\alpha 3}|^2$. In this case, the neutrino flux at Earth is $\Phi_{\text{inverted}} = \{|U_{e3}|^2, |U_{\mu3}|^2, |U_{\tau3}|^2\}$. Both Φ_{normal} and Φ_{inverted}, which are indicated by crosses ($\times$) in Figure 10, are very different from the standard flux $\Phi_{\text{std}} = \{\varphi_e = \frac{1}{3}, \varphi_\mu = \frac{1}{3}, \varphi_\tau = \frac{1}{3}\}$ produced by the ideal transfer matrix from a standard source. Observing either mixture would represent a departure from conventional expectations.

The fluxes that result from neutrino decays *en route* from the sources to Earth are subject to uncertainties in the neutrino-mixing matrix. The expectations for the two decay scenarios are indicated by the blue regions in Figure 10, where we indicate the consequences of 95% CL ranges of the mixing parameters now and in the future. With current uncertainties [101], the normal hierarchy populates $0.60 \lesssim \varphi_e \lesssim 0.73$, and allows considerable departures from $\varphi_\mu = \varphi_\tau$. The normal-hierarchy decay region based on current knowledge overlaps the flavor mixtures that
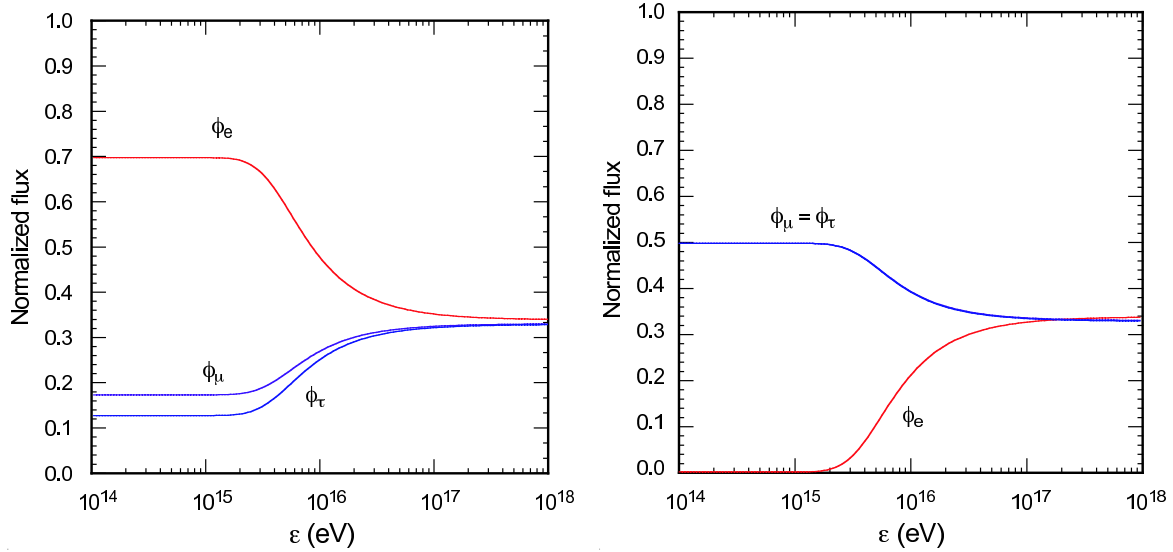
FIG. 12: Energy dependence of normalized ν_e, ν_μ, and ν_τ fluxes, for the two-body decay of the two upper mass eigenstates, with the neutrino source at $L = 100$ Mpc from Earth and $\tau/m = 1$ s/eV. The left pane shows the result for a normal mass hierarchy; the right pane shows the result for an inverted mass hierarchy. With suitable rescaling of the neutrino energy $[E_\nu = \varepsilon(1 \text{ s/eV})/(\tau_\nu/m_\nu) \cdot L/(100 \text{ Mpc})]$, these plots apply for any combination of path length and reduced lifetime [122].

oscillations produce in a pure-ν_e source, shown in orange. (It is, however, far removed from the standard region that encompasses Φ_{std}.) With the projected tighter constraints on the mixing angles, the range in φ_e swept out by oscillation from a pure-ν_e source or decay from a normal hierarchy shrinks by about a factor of two, and is separated from the oscillations. The degree of separation between the region populated by normal-hierarchy decay and the one populated by mixing from a pure-ν_e source depends on the value of the solar mixing angle θ_{12}. For the apparently excluded value $\theta_{12} = \frac{\pi}{4}$, both mechanisms would yield $\Phi = \{\frac{1}{2}, \frac{1}{4}, \frac{1}{4}\}$.

The mixtures that result from the decay of the heavier members of an inverted hierarchy entail $\varphi_e \approx 0$. These mixtures are well separated from any that would result from neutrino oscillations, for any conceivable source at cosmic distances.

The energies of neutrinos that may be detected in the future from AGNs and other cosmic sources range over several orders of magnitude, whereas the distances to such sources vary over perhaps one order of magnitude. The neutrino energy sets the neutrino lifetime in the laboratory frame; more energetic neutrinos survive over longer flight paths than their lower-energy companions. [A similar phenomenon is familiar for cosmic-ray muons.] Under propitious circumstances of reduced lifetime, path length, and neutrino energy, it might be possible to observe the transition from more energetic survivor neutrinos to less energetic decayed neutrinos.

If decay is not complete, the (unnormalized) flavor ν_α flux arriving at Earth from a source at distance L is $\widetilde{\varphi}_\alpha(E_\nu) = \sum_i \sum_\beta \varphi_\beta^0(E_\nu)|U_{\beta i}|^2|U_{\alpha i}|^2 e^{-(L/E_\nu)(m_i/\tau_i)}$, with the normalized flux $\varphi_\alpha(E_\nu) = \widetilde{\varphi}_\alpha(E_\nu)/\sum_\beta \widetilde{\varphi}_\beta(E_\nu)$. An idealized case will illustrate the possibilities for observing the onset of neutrino decay and estimating the reduced lifetime. Assume a normal mass hierarchy, $m_1 < m_2 < m_3$, and consider the special case $\tau_3/m_3 = \tau_2/m_2 \equiv \tau/m$. For a given path length L, the neutrino energy at which the transition occurs from negligible decays to complete decays is determined by τ/m. The left pane of Figure 12 shows the energy evolution of the normalized neutrino fluxes arriving from a standard source; the energy scale is appropriate for the case $\tau/m = 1$ s/eV and $L = 100$ Mpc.

If we locate the transition from survivors to decays at neutrino energy $E^\star$, then we can estimate the reduced lifetime in terms of the distance to the source as

$$\tau/m \approx 100 \text{ s/eV} \cdot \left(\frac{L}{1 \text{ Mpc}}\right)\left(\frac{1 \text{ TeV}}{E^\star}\right) . \tag{42}$$
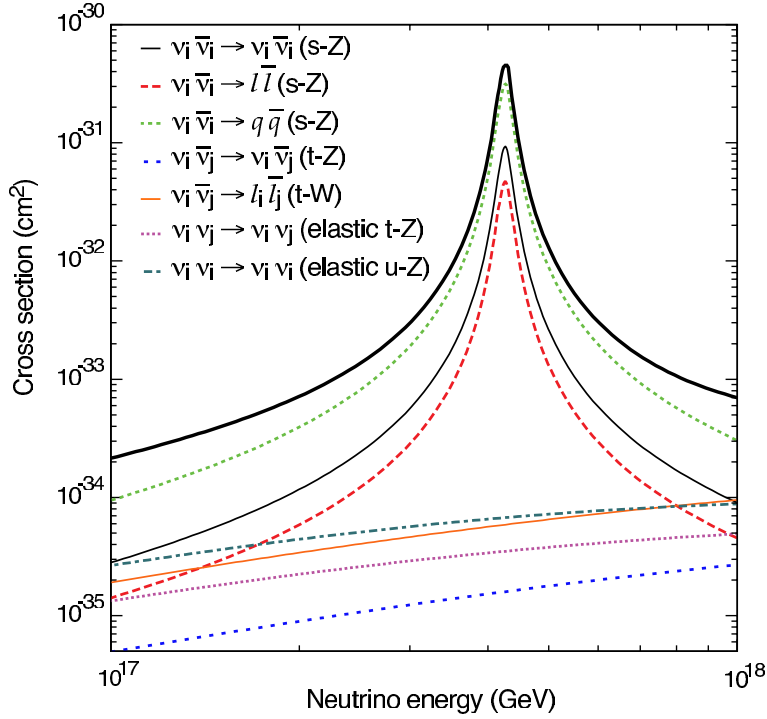
FIG. 13: Total neutrino annihilation cross section and the different contributing channels as a function of the neutrino energy assuming a relic neutrino mass of $m_\nu = 10^{-5}$ eV and zero redshift [61].

In practice, ultrahigh-energy neutrinos are likely to arrive from a multitude of sources at different distances from Earth, so the transition region will be blurred. Nevertheless, it would be rewarding to observe the decay-to-survival transition, and to use Eqn. (42) to estimate—even within one or two orders of magnitude—the reduced lifetime. If no evidence appears for a flavor mix characteristic of neutrino decay, then Eqn. (42) provides a lower bound on the neutrino lifetime. For that purpose, the advantage falls to large values of $L/E^\star$, and so to the lowest energies at which neutrinos from distant sources can be observed. Observing the standard flux, $\Phi_{\rm std} = \{\frac{1}{3}, \frac{1}{3}, \frac{1}{3}\}$, which is incompatible with neutrino decay, would strengthen the current bound on τ/m by some seven orders of magnitude, for 10-TeV neutrinos from sources at 100 Mpc.

IV.   NEUTRINO ABSORPTION SPECTROSCOPY

The neutrino gas that we believe permeates the present Universe has never been detected directly. The example of the $\bar{\nu}_e e^- \to W^-$ "Glashow resonance" [128] has motivated studies of the resonant annihilation of extremely-high-energy cosmic neutrinos on background neutrinos through the reaction $\nu\bar\nu \to Z^0$ [129, 130, 131, 132, 133, 134, 135, 136]. The components of the neutrino-(anti)neutrino cross sections are shown in Figure 13. The feature that matters is the Z^0-formation line that occurs near the resonant energy $E_\nu^{Z{\rm res}} = M_Z^2/2m_{\nu_i}$. The smallness of the neutrino masses (cf. Figure 4) means that the resonant energies are extremely high. If it were possible to observe Z-bursts or absorption lines, one could hope to confirm the presence of relic neutrinos and learn the absolute neutrino masses and the flavor composition of the neutrino mass eigenstates. To give an overview of the prospects for cosmic-neutrino annihilation spectroscopy, I summarize some of the main findings from a detailed study that Gabriela Barenboim, Olga Mena, and I carried out recently [61].

Imagine first a toy experiment, in which an extremely high-energy neutrino beam traverses a very long column with the relic-neutrino properties of the current Universe. Neglect for now the expansion of the Universe and the thermal motion of the relic neutrinos. The "cosmic neutrino attenuator" is thus a column of length L with uniform
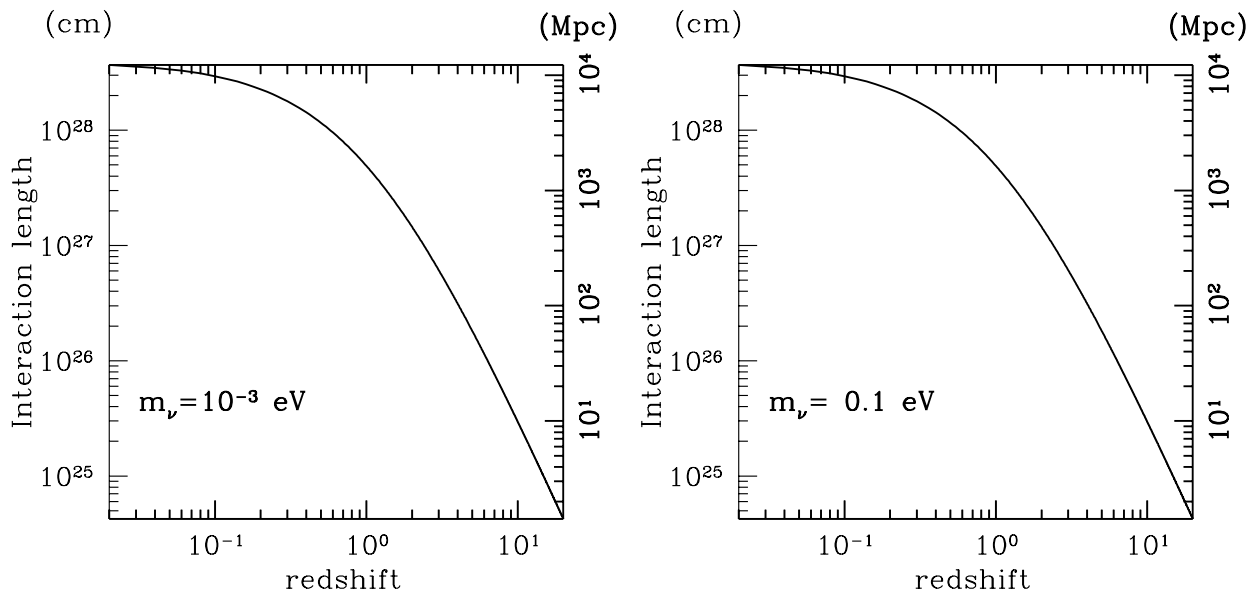
FIG. 14: Interaction lengths (for Dirac relic neutrinos) versus redshift at the Z^0 resonance for neutrino masses $m_\nu = 10^{-3}$ eV (left pane) and 10^{-1} eV (right pane). The left-hand scales are in centimeters, the right-hand scales in megaparsecs [61].

neutrino density $n_{\nu 0} = 56$ cm^{-3} of each neutrino species, $\nu_e, \bar{\nu}_e, \nu_\mu, \bar{\nu}_\mu, \nu_\tau, \bar{\nu}_\tau$. If the column of relic neutrinos is thick enough to attenuate neutrinos appreciably through resonant absorption at the Z^0 gauge boson, the energies that display absorption dips point to the neutrino masses through the resonant-energy condition. The relative depletion of ν_e, ν_μ, ν_τ in each of the lines measures the flavor composition of the corresponding neutrino mass eigenstate.

Even if we had at our disposal an adequate neutrino beam (with energies extending beyond 10^{26} eV), the time required to traverse one interaction length for $\nu\bar{\nu} \to Z^0$ annihilation on the relic background in the current Universe is 1.2×10^4 Mpc = 39 Gly. This exceeds the age of the Universe, not to mention the human attention span! If we are ever to detect the attenuation of neutrinos on the relic-neutrino background, we shall have to make use of astrophysical or cosmological neutrinos sources traversing the Universe over cosmic time scales. The expansion of the Universe over the propagation time of the neutrinos entails three important effects: the evolution of relic-neutrino density, the redshift of the incident neutrino energy, and the redshift of the relic-neutrino temperature.

In an evolving Universe, the column density of relic neutrinos is proportional to $(1 + z)^2/H(z)$, where z is the redshift and $H(z)$ is the Hubble parameter. The resulting decrease of interaction lengths with increasing redshift shown in Figure 14 reveals that for $1 \lesssim z \lesssim 10$, the interaction length matches the distance to the AGNs we consider as plausible UHE neutrino sources . . . though not perhaps with the energies required for this application. To compute the absorption lines, we must propagate ultrahigh-energy neutrinos through an evolving Universe.

The tiny neutrino mass makes for another complication: relic neutrinos are moving targets, with their momentum distribution characterized in the present Universe by Eq. (16). The thermal motion of the neutrinos gives rise to a Fermi (momentum) smearing of the UHE-ν–relic-ν cross section. The resonant incident-neutrino energy for a relic neutrino in motion is given by

$$E_\nu^{Z\mathrm{res}} = \frac{M_Z^2}{2(\varepsilon_\nu - p_\nu \cos\theta)} , \tag{43}$$

where p_ν and ε_ν are the relic-neutrino momentum and energy. The angle θ characterizes the direction of the relic neutrino with respect to the line of flight of the incident UHE neutrino. Accordingly, the resonant energy will be displaced downward from $M_Z^2/2m_\nu$ to approximately

$$\widetilde{E}_\nu^{Z\mathrm{res}} = \frac{M_Z^2}{2\langle\varepsilon_\nu\rangle} , \tag{44}$$
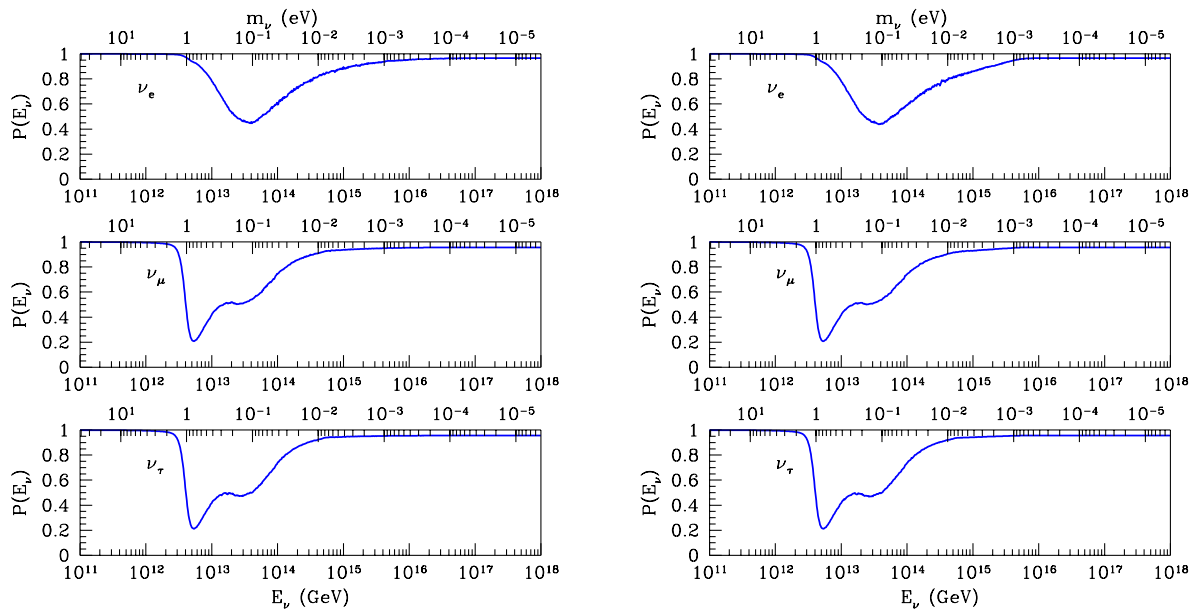
FIG. 15: Survival probabilities for ν_e, ν_μ, and ν_τ as a function of the neutrino energy, after integration back to redshift $z = 20$, taking into account the Fermi smearing induced by the thermal motion of the relic neutrinos. The results apply for a normal hierarchy with lightest neutrino mass $m_\ell = 10^{-5}$ eV (left pane) or $m_\ell = 10^{-3}$ eV (right pane) [61].

where $\langle \varepsilon_\nu \rangle = [\langle p_\nu^2 \rangle + m_\nu^2]^{1/2}$ plays the role of an *effective relic-neutrino mass*. The root-mean-square relic-neutrino momentum, which ranges from 6×10^{-4} eV in the present Universe to 2.5×10^{-2} eV at redshift $z = 20$, thus serves as a rough lower bound on the effective neutrino mass. At a given redshift, the resonance peak for scattering from any neutrino with $m_\nu \lesssim \langle \varepsilon_\nu \rangle$ will be changed significantly.

The absorption lines that result from a full calculation, including the effects of the relics' Fermi motion and the evolution of the Universe back to redshift $z = 20$, are shown in Figure 15 for two values of the lightest neutrino mass, $m_\ell = 10^{-5}$ and 10^{-3} eV. Although the lines are distorted and displaced from their natural shapes and positions by redshifting and Fermi motion, they would nevertheless confirm our expectations for the relic neutrino background and give important information about the neutrino spectrum. In particular, the ν_e/ν_μ ratio, shown in Figure 16, is a marker for the normal or inverted mass hierarchy.

At least in principle, the observation of cosmic-neutrino absorption lines would open the way to new insights about neutrino properties and the thermal history of the universe. How the tale unfolds will depend on factors we cannot foresee. The earlier in redshift the relevant cosmic-neutrino sources appear, the lower the present-day energy of the absorption lines and the denser the column of relics the super-high-energy neutrinos must traverse. In particular, the appearance of dips at energies much lower that we expect points to early—presumably nonacceleration—sources, that could give us insight into fundamental physics at early times and high energy scales. On the other hand, integration over a longer range in redshift means more smearing and distortion of the absorption lines.

If it can be achieved at all, the detection of neutrino absorption lines will not be done very soon, and the interpretation is likely to require many waves of observation and analysis. Nevertheless, observations of cosmic-neutrino absorption lines offer the possibility to establish the existence of another relic from the big bang and, conceivably, they may open a window on periods of the thermal history of the universe not readily accessible by other means.

V. CONCLUDING REMARKS

Just as new revelations about neutrino properties are enriching our understanding of particle physics, neutrino astronomy, astrophysics, and cosmology are blossoming. In this short tour, I have had to omit many topics of interest,
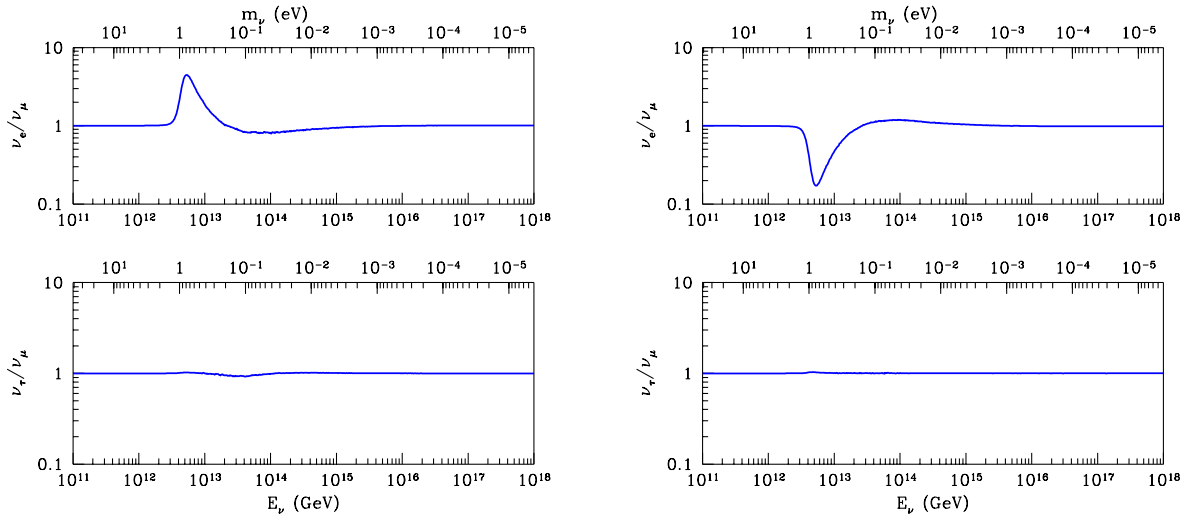
FIG. 16: Flux ratios ν_e/ν_μ and ν_τ/ν_μ at Earth, for normal (left pane) and inverted (right pane) mass hierarchies with $m_\ell = 10^{-5}$ eV, after integration back to redshift $z = 20$ and a thermal averaging over the relic-neutrino momentum distribution. The scale at the top shows the neutrino mass defined as $m_\nu = M_Z^2/2E_\nu$ that would be inferred if neutrino energies were not redshifted [61].

so I close with a short guide to the literature on some of the neglected topics.

The rôle of light neutrinos in cosmology was explored early on [137], and at a certain moment the possibility of a neutrino-dominated Universe had some currency [138]. Joel Primack reviewed the progression of dark-matter candidates, neutrinos included, in his SSI lecture [139].

We now expect neutrinos to contribute a dash of hot dark matter to the composition of the Universe. Neutrinos may signal dark-matter annihilations at the center of our galaxy [140, 141, 142, 143, 144], but rates may be unobservably small without a significant boost from dark-matter clumping [145]. The connection between dark matter and collider physics is emphasized in [146, 147]. Coannihilation of cosmic neutrinos on dark-matter particles appears to be a negligible source of indirect dark-matter signals [148].

Neutrinos may be relevant to two outstanding challenges in cosmology. Under the right circumstances, a lepton–antilepton asymmetry in the early Universe drive the matter excess we observe today. The leptogenesis scenario is reviewed in [67, 149, 150]. Mass varying neutrinos can behave as a negative-pressure fluid that could be the origin of the accelerated expansion of the Universe [151, 152, 153]. This approach aims to correlate the range of neutrino masses suggested by neutrino-oscillation experiments with the scale of the cosmological constant employed to parametrize the cosmic acceleration, $\Lambda \approx (\text{a few meV})^4$.

Acknowledgments

understanding of neutrino flavor change and for helpful comments on the manuscript.

---

[1] L. M. Krauss, S. L. Glashow, and D. N. Schramm, Nature **310**, 191 (1984).

[2] F. Mantovani, L. Carmignani, G. Fiorentini, and M. Lissia, Phys. Rev. **D69**, 013001 (2004), `hep-ph/0309013`.

[3] T. Araki et al., Nature **436**, 499 (2005).

[4] G. Duda, G. Gelmini, and S. Nussinov, Phys. Rev. **D64**, 122001 (2001), `hep-ph/0107027`.

[5] A. Ringwald and Y. Y. Y. Wong, JCAP **0412**, 005 (2004), `hep-ph/0408241`.

[6] A. G. Cocco, G. Mangano, and M. Messina, JCAP **0706**, 015 (2007), `hep-ph/0703075`.

[7] T. Han and D. Hooper, New J. Phys. **6**, 150 (2004), `hep-ph/0408348`.

[8] W.-M. Yao et al. (Particle Data Group), J. Phys. **G33**, 1 (2006), and 2007 partial update for 2008, URL `pdg.lbl.gov`.

[9] S. Dodelson (2007), *Cosmology for Particle Physicists,* Lectures at the 2007 SLAC Summer Institute, URL `www-conf.slac.stanford.edu/ssi/2007/`.

[10] J. Bahcall, *Neutrino Astrophysics* (Cambridge University Press, Cambridge & New York, 1989).

[11] C. Giunti and C. W. Kim, *Fundamentals of Neutrino Physics and Astrophysics* (Oxford University Press, Oxford & New York, 2007).

[12] S. Hannestad, Ann. Rev. Nucl. Part. Sci. **56**, 137 (2006), `hep-ph/0602058`.

[13] G. Mangano (2007), *Neutrinos in Cosmology,* Lectures at the III International Pontecorvo Neutrino Physics School, URL `www.jinr.ru/pontecorvo07/`.

[14] Fermilab–KEK Neutrino School (2007), URL `nuss.fnal.gov`.

[15] M. Yu. Khlopov, *Cosmoparticle Physics* (World Scientific, Singapore, 1999).

[16] G. Steigman, Int. J. Mod. Phys. **E15**, 1 (2006), `astro-ph/0511534`.

[17] B. D. Fields and S. Sarkar (2006), in [8], § 20, URL `pdg.lbl.gov/2007/reviews/bigbangnucrpp.pdf`.

[18] C. L. Bennett et al. (WMAP Collaboration), Astrophys. J. Suppl. **148**, 1 (2003), `astro-ph/0302207`.

[19] J. R. Bond, G. Efstathiou, and J. Silk, Phys. Rev. Lett. **45**, 1980 (1980).

[20] M. Tegmark, Phys. Scripta **T121**, 153 (2005), `hep-ph/0503257`.

[21] V. Barger, J. P. Kneller, H.-S. Lee, D. Marfatia, and G. Steigman, Phys. Lett. **B566**, 8 (2003), `hep-ph/0305075`.

[22] G. Steigman (2006), `astro-ph/0610599`.

[23] F. de Bernardis, A. Melchiorri, L. Verde, and R. Jimenez (2007), `arXiv:0707.4170`.

[24] S. S. Gershtein and Y. B. Zeldovich, JETP Lett. **4**, 120 (1966).

[25] R. Cowsik and J. McClelland, Phys. Rev. Lett. **29**, 669 (1972).

[26] G. L. Fogli et al., Phys. Rev. **D70**, 113003 (2004), `hep-ph/0408045`.

[27] Y. Fukuda et al. (Super-Kamiokande Collaboration), Phys. Rev. Lett. **81**, 1562 (1998), `hep-ex/9807003`.

[28] Q. R. Ahmad et al. (SNO Collaboration), Phys. Rev. Lett. **89**, 011301 (2002), `nucl-ex/0204008`.

[29] K. Eguchi et al. (KamLAND Collaboration), Phys. Rev. Lett. **90**, 021802 (2003), `hep-ex/0212021`.

[30] M. Goldhaber, L. Grodzins, and A. W. Sunyar, Phys. Rev. **109**, 1015 (1958).

[31] M. Bardon, P. Franzini, and J. Lee, Phys. Rev. Lett. **7**, 23 (1961).

[32] A. Possoz et al., Phys. Lett. **B70**, 265 (1977), erratum-ibid. **B73,** 504 (1978).

[33] K. Abe et al. (SLD Collaboration), Phys. Rev. Lett. **78**, 4691 (1997).

[34] C. Quigg (2007), *Neutrinos in the Electroweak Theory,* Lectures at the 2007 Fermilab/KEK Neutrino Physics Summer School, URL `lutece.fnal.gov/Talks/CQNuSchool.pdf`.

[35] S. Parke, in *Advanced Summer School in Physics 2006: Frontiers in Contemporary Physics: EAV06*, edited by O. Miranda et al. (American Institute of Physics, New York, 2007), pp. 69–84, AIP Conference Proceedings vol. 885, URL `link.aip.org/link/?APCPCS/885/69/1`.

[36] R. N. Mohapatra (2007), *Physics of Neutrino Mass,* Lectures at the 2007 Fermilab/KEK Neutrino Physics Summer School, URL `projects.fnal.gov/nuss/lectures/RabiM_1.pdf`.

[37] G. Drexlin (2006), *The KATRIN Experiment,* talk at the GERDA Collaboration Meeting, MPIK Heidelberg, URL `www-ik.fzk.de/~katrin/publications/talks/mpik2006.pdf`.

[38] G. G. Raffelt, Phys. Rev. D **31**, 3002 (1985).

[39] A. Mirizzi, D. Montanino, and P. D. Serpico, Phys. Rev. **D76**, 053007 (2007), `arXiv:0705.4667`.

[40] J. F. Beacom and N. F. Bell, Phys. Rev. **D65**, 113009 (2002), `hep-ph/0204111`.

[41] B. Kayser, ECONF **C040802**, L004 (2004), `hep-ph/0506165`.

[42] R. Davis, Rev. Mod. Phys. **75**, 985 (2003), URL `nobelprize.org/nobel_prizes/physics/laureates/2002/davis-lecture.html`.

[43] M. Koshiba, Rev. Mod. Phys. **75**, 1011 (2003), URL `nobelprize.org/nobel_prizes/physics/laureates/2002/koshiba-lecture.html`.

[44] A. Strumia and F. Vissani (2006–2008), "Neutrino masses and mixings and . . ." an organic review, the most recent version is available at `www.pi.infn.it/~astrumia/review.html`, `hep-ph/0606054`.

[45] K. S. Hirata et al. (Kamiokande-II Collaboration), Phys. Lett. **B280**, 146 (1992).

[46] Y. Ashie et al. (Super-Kamiokande Collaboration), Phys. Rev. **D71**, 112005 (2005), `hep-ex/0501064`.

[47] M. H. Ahn et al. (K2K Collaboration), Phys. Rev. **D74**, 072003 (2006), `hep-ex/0606032`.

[48] D. G. Michael et al. (MINOS Collaboration), Phys. Rev. Lett. **97**, 191801 (2006), `hep-ex/0607088`.

[49] MINOS Collaboration (2007), `arXiv:0708.1495`.

[50] Y. Ashie et al. (Super-Kamiokande Collaboration), Phys. Rev. Lett. **93**, 101801 (2004), `hep-ex/0404034`.

[51] T. Araki et al. (KamLAND Collaboration), Phys. Rev. Lett. **94**, 081801 (2005), `hep-ex/0406035`.

[52] S. Abe et al. (KamLAND Collaboration) (2008), `arXiv:0801.4589`.

[53] C. Arpesella et al. (Borexino Collaboration), Phys. Lett. **B658**, 101 (2008), `arXiv:0708.2251`.

[54] S. Fukuda et al. (Super-Kamiokande Collaboration), Phys. Rev. Lett. **86**, 5651 (2001), `hep-ex/0103032`.

[55] Q. R. Ahmad et al. (SNO Collaboration), Phys. Rev. Lett. **87**, 071301 (2001), `nucl-ex/0106015`.

[56] J. N. Bahcall, A. M. Serenelli, and S. Basu, Astrophys. J. **621**, L85 (2005), `astro-ph/0412440`.

[57] S. Fukuda et al. (Super-Kamiokande Collaboration), Phys. Lett. **B539**, 179 (2002), `hep-ex/0205075`.

[58] B. Aharmim et al. (SNO), Phys. Rev. **C72**, 055502 (2005), `nucl-ex/0502021`.

[59] A. A. Aguilar-Arevalo et al. (MiniBooNE Collaboration), Phys. Rev. Lett. **98**, 231801 (2007), `arXiv:0704.1500`.

[60] G. Steigman, Ann. Rev. Nucl. Part. Sci. **29**, 313 (1979).

[61] G. Barenboim, O. Mena Requejo, and C. Quigg, Phys. Rev. **D71**, 083002 (2005), `hep-ph/0412122`.

[62] R. E. Lopez, S. Dodelson, A. Heckler, and M. S. Turner, Phys. Rev. Lett. **82**, 3952 (1999), `astro-ph/9803095`.

[63] R. Cowsik and J. McClelland, Astrophys. J. **180**, 7 (1973).

[64] A. S. Szalay and G. Marx, Astron. Astrophys. **49**, 437 (1976).

[65] J. F. Beacom, N. F. Bell, and S. Dodelson, Phys. Rev. Lett. **93**, 121302 (2004), `astro-ph/0404585`.

[66] G. B. Gelmini, Phys. Scripta **T121**, 131 (2005), `hep-ph/0412305`.

[67] M. Fukugita, Nucl. Phys. Proc. Suppl. **155**, 10 (2006), `hep-ph/0511068`.

[68] C. Giunti and M. Laveder (2007), *Neutrino Mass Limits*, URL `www.nu.to.infn.it/Neutrino_Cosmology`.

[69] J. Lesgourgues and S. Pastor, Phys. Rept. **429**, 307 (2006), `astro-ph/0603494`.

[70] S. Dodelson (2007), *Neutrinos and the Universe—Cosmology,* Lecture at the 2007 Fermilab/KEK Neutrino Physics Summer School, URL `theory.fnal.gov/jetp/talks/dodelson.pdf`.

[71] M. Tegmark et al. (SDSS Collaboration), Phys. Rev. **D69**, 103501 (2004), `astro-ph/0310723`.

[72] D. N. Spergel et al. (WMAP Collaboration), Astrophys. J. Suppl. **170**, 377 (2007), `astro-ph/0603449`.

[73] A. Goobar, S. Hannestad, E. Mortsell, and H. Tu, JCAP **0606**, 019 (2006), `astro-ph/0602155`.

[74] A. Melchiorri, P. Serra, S. Dodelson, and A. Slosar, New Astron. Rev. **50**, 1020 (2006).

[75] U. Seljak, A. Slosar, and P. McDonald, JCAP **0610**, 014 (2006), `astro-ph/0604335`.

[76] M. Cirelli and A. Strumia, JCAP **0612**, 013 (2006), `astro-ph/0607086`.

[77] P. D. Serpico, Phys. Rev. Lett. **98**, 171301 (2007), `astro-ph/0701699`.

[78] A. R. Cooray, Astron. Astrophys. **348**, 31 (1999), `astro-ph/9904246`.

[79] S. M. Bilenky, C. Giunti, J. A. Grifols, and E. Massó, Phys. Rept. **379**, 69 (2003), `hep-ph/0211462`.

[80] S. F. King, Rept. Prog. Phys. **67**, 107 (2004), `hep-ph/0310204`.

[81] R. N. Mohapatra, ECONF **C040802**, L011 (2004), `hep-ph/0411131`.

[82] R. N. Mohapatra and A. Y. Smirnov, Ann. Rev. Nucl. Part. Sci. **56**, 569 (2006), `hep-ph/0603118`.

[83] S. F. King, Contemporary Physics **48**, 195 (2007), `arXiv:0712.1750`.

[84] S. R. Elliott and P. Vogel, Ann. Rev. Nucl. Part. Sci. **52**, 115 (2002), `hep-ph/0202264`.

[85] F. T. Avignone, III, S. R. Elliott, and J. Engel (2007), `arXiv:0708.1033`.

[86] F. Piquemal (2007), *Beta Decay Experiments,* talk at the XXIII International Symposium on Lepton and Photon Interactions at High Energies, URL `chep.knu.ac.kr/lp07/htm/S12/S12_36.pdf`.

[87] P. Vogel and A. Piepke (2007), in [8], URL `pdg.lbl.gov/2007/reviews/betabeta_s076.pdf`.

[88] G. B. Gelmini and M. Roncadelli, Phys. Lett. **B99**, 411 (1981).

[89] S. Weinberg, Phys. Rev. Lett. **43**, 1566 (1979).

[90] P. Minkowski, Phys. Lett. **B67**, 421 (1977).

[91] T. Yanagida, in *Proceedings of the Workshop on the Baryon Number of the Universe and Unified Theories*, edited by O. Sawada and A. Sugamoto (KEK, Tsukuba, 1979), pp. 95–98, [reprinted in *SEESAW 25: Proceedings of the International Conference on the Seesaw Mechanism* ed Orloff J, Lavignac S and Cribier M (Singapore: World Scientific, 2005) pp 261-264].

[92] M. Gell-Mann, P. Ramond, and R. Slansky, in *Supergravity*, edited by van Nieuwenhuizen, P. and D. Z. Freedman (North-Holland, Amsterdam, 1979), pp. 95–101.

[93] R. N. Mohapatra and G. Senjanovic, Phys. Rev. Lett. **44**, 912 (1980).

[94] J. Schechter and J. W. F. Valle, Phys. Rev. **D22**, 2227 (1980).

[95] A. Y. Smirnov, in *SEESAW 25: Proceedings of the International Conference on the Seesaw Mechanism*, edited by J. Orloff, S. Lavignac, and M. Cribier (World Scientific, Singapore, 2005), pp. 221–236, `hep-ph/0411194`.

[96] M.-C. Chen, A. de Gouvêa, and B. A. Dobrescu, Phys. Rev. **D75**, 055009 (2007), `hep-ph/0612017`.

[97] B. W. Lee and R. E. Shrock, Phys. Rev. **D16**, 1444 (1977).

[98] B. Pontecorvo, Zh. Eksp. Teor. Fiz. **34**, 247 (1957), [English transl.: *Sov. Phys. JETP* **7** 172-173 (1958)].

[99] Z. Maki, M. Nakagawa, and S. Sakata, Prog. Theor. Phys. **28**, 870 (1962).

[100] M. C. Gonzalez-Garcia, Phys. Scripta **T121**, 72 (2005), `hep-ph/0410030`.

[101] M. C. Gonzalez-Garcia and M. Maltoni (2007), `arXiv:0704.1800`.

[102] M. Maltoni, T. Schwetz, M. A. Tortola, and J. W. F. Valle, New J. Phys. **6**, 122 (2004), `hep-ph/0405172v6`.

[103] M. Ackermann et al. (IceCube Collaboration) (2007), `arXiv:0711.3022`.

[104] I. F. M. Albuquerque (2006), `hep-ph/0612090`.

[105] K. Hoffman (2007), *Recent Results from AMANDA and Prospects for IceCube,* Topical Conference Lecture at the 2007 SLAC Summer Institute, URL `www-conf.slac.stanford.edu/ssi/2007/`.

[106] Y. M. Andreev, V. S. Berezinsky, and A. Y. Smirnov, Phys. Lett. **B84**, 247 (1979).

[107] E. Eichten, I. Hinchliffe, K. D. Lane, and C. Quigg, Rev. Mod. Phys. **56**, 579 (1984).

[108] C. Quigg, M. H. Reno, and T. P. Walker, Phys. Rev. Lett. **57**, 774 (1986).

[109] M. H. Reno and C. Quigg, Phys. Rev. **D37**, 657 (1988).

[110] R. Gandhi, C. Quigg, M. H. Reno, and I. Sarcevic, Astropart. Phys. **5**, 81 (1996), `hep-ph/9512364`.

[111] R. Gandhi, C. Quigg, M. H. Reno, and I. Sarcevic, Phys. Rev. **D58**, 093009 (1998), `hep-ph/9807264`.

[112] M. H. Reno, Nucl. Phys. Proc. Suppl. **143**, 407 (2005), `hep-ph/0410109`.

[113] A. Cooper-Sarkar and S. Sarkar, JHEP **01**, 075 (2008), `arXiv:0710.5303`.

[114] J. Pumplin et al. (CTEQ Collaboration), JHEP **07**, 012 (2002), `hep-ph/0201195`.

[115] E. L. Berger, M. M. Block, D. W. McKay, and C.-I. Tan (2007), `arXiv:0708.1960`.

[116] C. Adloff et al. (H1 Collaboration), Eur. Phys. J. **C30**, 1 (2003), `hep-ex/0304003`.

[117] S. Chekanov et al. (ZEUS Collaboration), Phys. Rev. **D67**, 012007 (2003), `hep-ex/0208023`.

[118] S. Chekanov et al. (ZEUS Collaboration), Eur. Phys. J. **C49**, 523 (2007), `hep-ex/0608014`.

[119] L. A. Anchordoqui, A. M. Cooper-Sarkar, D. Hooper, and S. Sarkar, Phys. Rev. **D74**, 043008 (2006), `hep-ph/0605086`.

[120] J. G. Learned and S. Pakvasa, Astropart. Phys. **3**, 267 (1995), `hep-ph/9405296`.

[121] P. C. de Holanda and A. Y. Smirnov, JCAP **0302**, 001 (2003), `hep-ph/0212270`.

[122] G. Barenboim and C. Quigg, Phys. Rev. **D67**, 073024 (2003), `hep-ph/0301220`.

[123] T. Kashti and E. Waxman, Phys. Rev. Lett. **95**, 181101 (2005), `astro-ph/0507599`.

[124] J. W. F. Valle, Phys. Lett. **B131**, 87 (1983).

[125] G. B. Gelmini and J. W. F. Valle, Phys. Lett. **B142**, 181 (1984).

[126] J. F. Beacom, N. F. Bell, D. Hooper, S. Pakvasa, and T. J. Weiler, Phys. Rev. Lett. **90**, 181301 (2003), `hep-ph/0211305`.

[127] Z. Chacko, L. J. Hall, T. Okui, and S. J. Oliver, Phys. Rev. **D70**, 085008 (2004), `hep-ph/0312267`.

[128] S. L. Glashow, Phys. Rev. **118**, 316 (1960).

[129] T. J. Weiler, Phys. Rev. Lett. **49**, 234 (1982).

[130] T. J. Weiler, Astrophys. J. **285**, 495 (1984).

[131] E. Roulet, Phys. Rev. **D47**, 5247 (1993).

[132] P. Gondolo, G. Gelmini, and S. Sarkar, Nucl. Phys. **B392**, 111 (1993), `hep-ph/9209236`.

[133] S. Yoshida, H.-y. Dai, C. C. H. Jui, and P. Sommers, Astrophys. J. **479**, 547 (1997), `astro-ph/9608186`.

[134] D. Fargion, B. Mele, and A. Salis, Astrophys. J. **517**, 725 (1999), `astro-ph/9710029`.

[135] T. J. Weiler, Astropart. Phys. **11**, 303 (1999), `hep-ph/9710431`.

[136] B. Eberle, A. Ringwald, L. Song, and T. J. Weiler, Phys. Rev. **D70**, 023007 (2004), `hep-ph/0401203`.

[137] S. Tremaine and J. E. Gunn, Phys. Rev. Lett. **42**, 407 (1979).

[138] D. N. Schramm and G. Steigman, Gen. Rel. Grav. **13**, 101 (1981).

[139] J. Primack (2007), *A Brief History of Dark Matter,* Lecture at the 2007 SLAC Summer Institute, URL `www-conf.slac.stanford.edu/ssi/2007/`.

[140] G. Bertone, D. Hooper, and J. Silk, Phys. Rept. **405**, 279 (2005), `hep-ph/0404175`.

[141] P. Gondolo et al., JCAP **0407**, 008 (2004), `astro-ph/0406204`.

[142] M. Cirelli et al., Nucl. Phys. **B727**, 99 (2005), `hep-ph/0506298v3`.

[143] R. Lehnert and T. J. Weiler (2007), `arXiv:0708.1035`.

[144] V. Barger, W.-Y. Keung, G. Shaughnessy, and A. Tregre (2007), `arXiv:0708.1325`.

[145] V. Berezinsky, V. Dokuchaev, and Y. Eroshenko, Phys. Rev. **D68**, 103003 (2003), `astro-ph/0301551`.

[146] M. S. Carena, D. Hooper, and A. Vallinotto, Phys. Rev. **D75**, 055010 (2007), `hep-ph/0611065`.

[147] M. E. Peskin (2007), `arXiv:0707.1536`.

[148] G. Barenboim, O. Mena Requejo, and C. Quigg, Phys. Rev. **D74**, 023006 (2006), `astro-ph/0604215`.

[149] W. Buchmuller, R. D. Peccei, and T. Yanagida, Ann. Rev. Nucl. Part. Sci. **55**, 311 (2005), `hep-ph/0502169`.

[150] M.-C. Chen (2007), lectures at *TASI 2006: Exploring New Frontiers Using Colliders and Neutrinos*, `hep-ph/0703087`.

[151] P. Q. Hung (2000), `hep-ph/0010126`.

[152] R. Fardon, A. E. Nelson, and N. Weiner, JCAP **0410**, 005 (2004), `astro-ph/0309800`.

[153] D. B. Kaplan, A. E. Nelson, and N. Weiner, Phys. Rev. Lett. **93**, 091801 (2004), `hep-ph/0401099`.